

FROM BLUE STAR-FORMING TO RED PASSIVE: GALAXIES IN TRANSITION IN DIFFERENT ENVIRONMENTS

BENEDETTA VULCANI¹, BIANCA M. POGGIANTI², JACOPO FRITZ^{3,4}, GIOVANNI FASANO², ALESSIA MORETTI^{2,5}, ROSA CALVI⁵, AND ANGELA PACCAGNELLA⁵

¹Kavli Institute for the Physics and Mathematics of the Universe (WPI), Todai Institutes for Advanced Study, the University of Tokyo, Kashiwa, 277-8582, Japan

²INAF - Astronomical Observatory of Padova, 35122 Padova, Italy

³Sterrenkundig Observatorium Vakgroep Fysica en Sterrenkunde Universiteit Gent, Krijgslaan 281, S9 9000 Gent, Belgium

⁴Centro de Radioastronomía y Astrofísica, CRYA, UNAM, Campus Morelia, A.P. 3-72, C.P. 58089 Michoacán, Mexico and

⁵Dipartimento di Astronomia, vicolo Osservatorio 2, 35122 Padova, Italy

Draft version October 27, 2014

ABSTRACT

Exploiting a mass complete ($M_* > 10^{10.25} M_\odot$) sample at $0.03 < z < 0.11$ drawn from the Padova Millennium Galaxy Group Catalog (PM2GC), we use the $(U - B)_{rf}$ color and morphologies to characterize galaxies, in particular those that show signs of an ongoing or recent transformation of their star formation activity and/or morphology - green galaxies, red passive late types, and blue star-forming early types. Color fractions depend on mass and only for $M_* < 10^{10.7} M_\odot$ on environment. The incidence of red galaxies increases with increasing mass, and, for $M_* < 10^{10.7} M_\odot$, decreases toward the group outskirts and in binary and single galaxies. The relative abundance of green and blue galaxies is independent of environment, and increases monotonically with galaxy mass. We also inspect galaxy structural parameters, star-formation properties, histories and ages and propose an evolutionary scenario for the different subpopulations. Color transformations are due to a reduction and suppression of SFR in both bulges and disks which does not noticeably affect galaxy structure. Morphological transitions are linked to an enhanced bulge-to-disk ratio due to the removal of the disk, not to an increase of the bulge. Our modeling suggests that green colors might be due to star formation histories declining with long timescales, as an alternative scenario to the classical “quenching” processes. Our results suggest that galaxy transformations in star formation activity and morphology depend neither on environment nor on being a satellite or the most massive galaxy of a halo. The only environmental dependence we find is the higher fast quenching efficiency in groups giving origin to post-starburst signatures.

Subject headings: galaxies: general – galaxies: formation – galaxies: evolution – galaxies: morphologies

1. INTRODUCTION

Galaxy color and structure are key observables in extragalactic astronomy for understanding the formation and evolution of galaxies, and they are the consequence of all physical processes at work.

The local population of galaxies consists roughly of two types, and their frequency correlates with the environment: red galaxies, which on the whole are characterized by larger stellar masses, bulge-dominated morphologies, are predominant in dense regions, while blue galaxies, with a disk-dominated morphology, are preferentially found in low density regions (Blanton *et al.* 2003; Kauffmann *et al.* 2003, 2004; Baldry *et al.* 2004; Balogh *et al.* 2004; Brinchmann *et al.* 2004). Since only relatively small amounts of ongoing star formation make a galaxy appear blue, the color bimodality basically reflects star formation quenching: in general, red galaxies have had their star formation quenched, while blue galaxies are still forming stars. However, a non-negligible fraction of red galaxies are clearly edge-on disc objects that owe their color to an enhanced extinction, and a small fraction of blue galaxies might have already stopped their activity (see, e.g., Bamford *et al.* 2009; Schawinski *et al.* 2009).

The bimodality can originate both from a priori differences set beforehand, the so-called nature scenario, or from environmentally driven processes taking place during the evolution of galaxies, the so-called nurture scenario. As discussed in De Lucia *et al.* (2012), trying to separate the two frameworks and differentiate their role in driving galaxy evolution might be an ill posed task, since they are strongly and physically

connected. According to the Λ CDM model, as time goes by, smaller structures merge to form progressively larger ones. This hierarchical growth implies that the fraction of galaxies located in groups progressively increases since $z \sim 1.5$, and at $z \sim 0$ most galaxies are found in groups (Huchra & Geller 1982; Eke *et al.* 2004; Berlind *et al.* 2006; Knobel *et al.* 2009). It is therefore important to understand the role of the group environment in boosting galaxy transformations from blue to red colors and from late- to early-type morphologies. Color and morphological fractions are very different functions of environment at low- z (Bamford *et al.* 2009). Being both sensitive to stellar mass, at fixed stellar mass, color is also highly sensitive to environment, while morphology displays much weaker environmental trends (see also Kauffmann *et al.* 2004; Blanton *et al.* 2005; Christlein & Zabludoff 2005; Weinmann *et al.* 2009; Kovač *et al.* 2010).

The existence of a variety of “sub-populations” of galaxies whose color does not correspond to what is expected based on their morphology (red late-types, blue early-types, etc) suggests that galaxy transformations from blue to red must occur on significantly shorter time-scales than transformations from late to early-type.

However, what drives the observed trends remains still not fully understood. Numerous processes may be responsible for the dependence of galaxy properties on environment (Boselli & Gavazzi 2006 and references therein). The extreme local densities reached within cluster cores enable efficient ram pressure stripping of the galaxy cold gas on timescales of a few Myr (Gunn & Gott 1972; Abadi, Moore & Bower 1999). On the other hand, galaxy-group interactions like “strangu-

lation” can remove warm and hot gas from a galaxy halo, efficiently cutting off the star formation gas supply (Larson, Tinsley & Caldwell 1980; Cole *et al.* 2000; Balogh, Navarro & Morris 2000; Kawata & Mulchaey 2008). Halos can play a role through tidal forces and dynamical friction. Galaxy-galaxy harassment at the typical velocity dispersion of bound groups and clusters may also result in star-formation quenching (Moore *et al.* 1996). Shock heating in massive halos can prevent accretion of cold gas that would feed star formation. Interactions and mergers can also apply torques that drive gas inward, perhaps feeding and then exhausting star formation or a central black hole.

Radial trends of galaxy properties (e.g., colors, morphologies) as a function of distance from the halo center can be observable effects of these processes responsible for the galaxy transformations. They have been extensively studied in galaxy clusters, where e.g., a strong radial dependence in the star-formation rate is observed (Hashimoto & Oemler 1999; Balogh *et al.* 1999; Lewis *et al.* 2002; Balogh *et al.* 2004; Tanaka *et al.* 2004; von der Linden *et al.* 2010).

Another way to gain insight into the physical processes is to study those galaxies whose morphological type places them on one side of the bimodality but whose star formation identifies them with the other. Blue early-type galaxies with high current star formation rates ($0.5 < \text{SFR} < 50 M_{\odot}/\text{yr}$) or a recently stopped star formation activity are one example (e.g., Kannappan, Guie & Baker 2009; Ferreras *et al.* 2009; Schawinski *et al.* 2009). These galaxies tend to live in lower density environments than red sequence early types and make up $\sim 6\%$ of the low- z general field early-type galaxy population. They might be early-type galaxies previously on the red sequence that are undergoing an episode of star formation due to the sudden availability of cold gas (“rejuvenated”), making them leave the red sequence before rejoining it. The gas might become available after a merger. If merging occurs between gas-rich galaxies, it may produce a larger amount of star formation (wet mergers), and transform disc galaxies into elliptical galaxies (Lin *et al.* 2008).

Another example of objects in transition is given by red late types. Their distribution displays a clear trend with both local density and group-centric distance: their fraction increases with increasing local density or decreasing group-centric distance, but at very high densities or in the cores of groups the red late-type fraction declines sharply (Bamford *et al.* 2009; Masters *et al.* 2010; van der Wel *et al.* 2009). Many of them have some ongoing star formation, and are reddened by dust extinction (e.g. Gallazzi *et al.* 2009; Wolf *et al.* 2009). They might be the result of quite gentle processes (e.g., galaxy-galaxy interactions, interaction with the inter galactic medium (IGM), harassment, strangulation, bar instabilities) that might allow the existence of the spiral structure even shutting down the star formation (e.g. Walker, Mihos & Hernquist 1996; Skibba & Sheth 2009; Skibba *et al.* 2009).

Aim of this study is characterize in detail the incidence of galaxies of different types in the local universe, and depict objects in transition, whose analysis will help us to shed light on the processes acting on galaxies and the time scale needed to galaxies to transform from one type to the other.

First, we study colors and morphologies of galaxies in different environments. Since many galaxy characteristics are interrelated (Cowie *et al.* 1996; Gavazzi, Pierini & Boselli 1996; Blanton *et al.* 2003; Kauffmann *et al.* 2003; Brinchmann *et al.* 2004; Baldry *et al.* 2004), we study the correlations for each property independently while fixing other

variables. When constraining environmental effects, we perform the analysis in different galaxy stellar mass bins. Galaxy colors and morphologies also correlate, so we split galaxies simultaneously by color and morphological types to distinguish between processes that affect star formation rates and structural properties differently. Second, we focus on objects in transition and study in detail their properties, with the aim to understand the evolutive scenario of these galaxies.

The analysis has been carried out using a cosmology with $(\Omega_m, \Omega_{\Lambda}, h) = (0.3, 0.7, 0.7)$, Vega magnitudes (unless otherwise stated) and a Kroupa (2001) Initial Mass Function (IMF).

2. THE DATA SET AND DATA SAMPLE

We use the Padova-Millennium Galaxy and Group Catalogue (PM2GC - Calvi, Poggianti & Vulcani 2011), consisting of a spectroscopically complete sample of galaxies at $0.03 \leq z \leq 0.11$ brighter than $M_B = -18.7$. This sample is sourced from the Millennium Galaxy Catalogue (MGC; Liske *et al.* 2003; Driver *et al.* 2005), a B-band contiguous equatorial survey of $\sim 38 \text{ deg}^2$ complemented by a 96% spectroscopically complete survey down to $B = 20$ and it is representative of the general field population in the local Universe.

By applying a friends-of-friends (FoF) algorithm, Calvi, Poggianti & Vulcani (2011) identified 176 galaxy groups with at least three members with $M_B < -18.7$ in the redshift range $0.04 \leq z \leq 0.1$. A galaxy is considered a group member if its spectroscopic redshift lies within $\pm 3\sigma$ (velocity dispersion) from the median group redshift and if it is located within a projected distance of $1.5R_{200}$ from the group geometrical center, where R_{200}^1 is defined as the radius delimiting a sphere with interior mean density 200 times the critical density of the universe at that redshift, and is commonly used as an approximation of the group virial radius. Galaxies that have no neighbors or just one with a projected mutual distance $0.5 h^{-1}$ Mpc and a redshift within 1500 km s^{-1} are considered “single” or “binary-system” galaxies, respectively.

Applying a FoF to the De Lucia & Blaizot (2007) semi-analytic model (Vulcani *et al.* 2014), we found that 80% of our group/binary systems/single galaxies span a halo mass range of $10^{12} - 10^{14} M_{\odot} / 10^{11.4} - 10^{12.6} M_{\odot} / 10^{11.2} - 10^{12.3} M_{\odot}$.

Rest-frame absolute magnitudes are computed using INTEREST (Taylor *et al.* 2009) from the observed SDSS photometry. The code uses a number of template spectra to carry out the interpolation from the observed photometry in bracketing bands (see Rudnick *et al.* 2003). Rest-frame colors are derived from the interpolated rest-frame apparent magnitudes.

Stellar masses are estimated following the Bell & de Jong (2001) relation (Calvi, Poggianti & Vulcani 2011), which correlates the stellar mass-to-light ratio with the optical colors of the integrated stellar population, using the B-band photometry taken from the MGC, and the rest-frame $B - V$ color computed from the Sloan $g - r$ color corrected for Galactic extinction:

$$\log_{10}(M/L_B) = -0.51 + 1.45(B - V) \quad (1)$$

valid for a Bruzual & Charlot model with solar metallicity and a Salpeter (1955) IMF ($0.1\text{--}125 M_{\odot}$). Then, they are converted to a Kroupa (2001) IMF, adding -0.19 dex to the logarithmic value of the masses (Cimatti *et al.* 2008). The typical uncertainty on mass estimates is $0.2\text{--}0.3$ dex (for details and comparisons with external estimates refer to Calvi, Poggianti

¹ The R_{200} values are computed from the velocity dispersions as in Finn *et al.* (2005).

& Vulcani 2011; Poggianti *et al.* 2013). The sample is complete for $\log M_*/M_\odot > 10.25$, corresponding to the mass of the faintest and reddest galaxy ($M_B = -18.7$, $B - V = 0.9$) at our redshift upper limit ($z=0.1$), as described in Calvi *et al.* (2012).

Star formation rates (SFR) and histories (SFH) are derived by fitting the spectra with the spectrophotometric model fully described in Fritz *et al.* (2007, 2011). The MGC spectroscopic database of PM2GC galaxies consists of SDSS, 2dFGRS and MGCz spectra (Driver *et al.* 2005), the latter taken with the same instrument and setup of the 2dFGRS. Choosing always the highest quality spectrum available, SDSS spectra are preferred when possible (86% of the sample), alternatively 2dFGRS spectra when available (12%) and MGCz spectra in the remaining cases. In the Fritz *et al.* (2007) model, all the main spectrophotometric features (i.e. the continuum flux and shape, the equivalent widths of emission and absorption lines) are reproduced by summing the theoretical spectra of simple stellar populations (SSP) of 12 different ages (from 3×10^6 to $\sim 14 \times 10^9$ years). The spectral analysis allows to derive an estimate of the SFRs at different cosmic times and of the average age of the stars in a galaxy.

Morphologies are determined using MORPHOT (Fasano *et al.* 2012), an automatic tool designed to reproduce as closely as possible the visual classifications. MORPHOT adds to the classical CAS (concentration/asymmetry/clumpiness) parameters a set of additional indicators derived from digital imaging of galaxies and has been proved to give an uncertainty only slightly larger than the eyeball estimates. It was applied to the B-band MGC images to identify ellipticals, lenticulars (S0s), and later-type galaxies (Calvi *et al.* 2012).

Structural parameters are taken from the public catalog of the MGC database (Allen *et al.* 2006), and were derived from 2D surface brightness profile fitting of MGC-BRIGHT galaxies using GIM2D (Simard *et al.* 2002). We use the catalog obtained adopting a bulge-disk decomposition model using a Sérsic bulge plus exponential disc. As described in Allen *et al.* (2006), the components were required to have a common spatial centre, but their luminosities were independent, allowing the calculation of a bulge-to-total (B/T) luminosity ratio for each galaxy. We refer to the original paper for additional details.

In this paper, we consider two galaxy classes and treat separately the most massive galaxy (MMG) of each structure and all the other galaxies, called satellites, regardless of environment. With this definition, all single galaxies are treated as MMGs, while binary systems are split into one MMG and one satellite. In addition, we remove AGNs, since their presence might alter results. To do that, we match our sample with the latest AGN catalog from SDSS,² finding that overall 48 galaxies that enter our entire mass complete sample are indeed hosting an AGN. Applying the fraction of AGN obtained ($< 4\%$) to the PM2GC subsample without spectra from SDSS, we expect ~ 9 AGN not detected above our mass completeness limit. We assume that this number is negligible.

The final mass complete sample of galaxies in groups consists of 417 satellites and 165 MMGs. The final binary system and single galaxy samples consist of 228 (170 of which are MMGs) and 418 galaxies respectively.

3. GALAXY SUB-POPULATIONS

Broadly speaking, based on color, galaxies can be subdivided into two populations: red and blue. To start, we plot

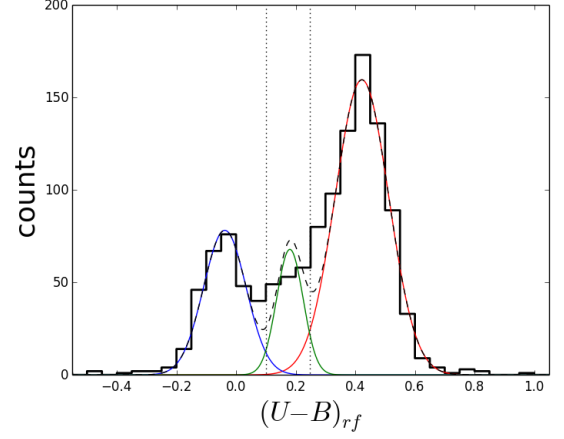


FIG. 1.— Rest frame $(U-B)_{rf}$ color distribution of all galaxies in our mass complete sample. Also plotted are Gaussian fits to the red, blue, green (solid lines) and total (black dashed line) population. The vertical lines indicate where gaussian fits intersect.

the $(U-B)_{rf}$ distribution of all galaxies above the mass completeness limit. Figure 1 highlights the presence of the well known bimodality, but also of an emerging third population, located in between the main peaks. We will refer to these as “green” galaxies. We fit the entire distribution with three Gaussian functions, to define the boundaries of the green population so it has the minimal overlap with the red and blue sequences. The position of the peaks depends on mass and redshift, so in principle, we should fit the color distribution at different stellar masses and in different redshift bins and then interpolate to find a relation that depends on stellar mass, color, redshift. Since no significant evolution is expected between $z \sim 0.1$ and $z \sim 0.04$, we neglect the redshift dependence. Given that our mass range is quite small, we can not compute the dependence of the cut on stellar mass, and we adopt the slope of the color-mass relation presented in Peng *et al.* (2010) (0.075). To compute the zero-points of the relations that separate different colors, we focus on the mass bin $M_* = 10^{10.5-11} M_\odot$ and find the values where the blue and green, green and red gaussians intersect each other. Galaxies are assigned to the red sequence if their rest-frame color obeys

$$(U-B)_{\text{vega}} \geq 0.075 \times \log M_* - 0.561 \quad (2)$$

to the blue cloud if their rest-frame color obeys

$$(U-B)_{\text{vega}} \leq 0.075 \times \log M_* - 0.709 \quad (3)$$

and to the green valley if they are in between the two cuts. This is visually shown in the upper panel of Fig. 2, where we plot also galaxies that do not enter our mass complete sample, just to show the general trends.

Table 1 presents the percentage of galaxies of different types and colors in different environments for the mass complete samples. The majority of galaxies are red, and more so for satellites ($\sim 70\%$) than MMGs ($\sim 60\%$). Green galaxies are 14% of all MMGs and 9% of all satellites, while blue galaxies are 26% of MMGs and 19% of satellites.

Color fractions strongly depend on environment (singles, binaries, groups), and not on galaxy class, that of MMGs and satellites being always compatible within the errors. Interestingly, green galaxies are always about half as numerous as blue galaxies, showing that their relative number is independent both of environment and of the distinction satellites-MMGs (see §4.1 for more details).

Considering morphologies, late types dominate both galaxy classes, being $\sim 40\%$ and $\sim 50\%$ of all satellites and MMGs,

² https://www.sdss3.org/dr10/spectro/spectro_access.php

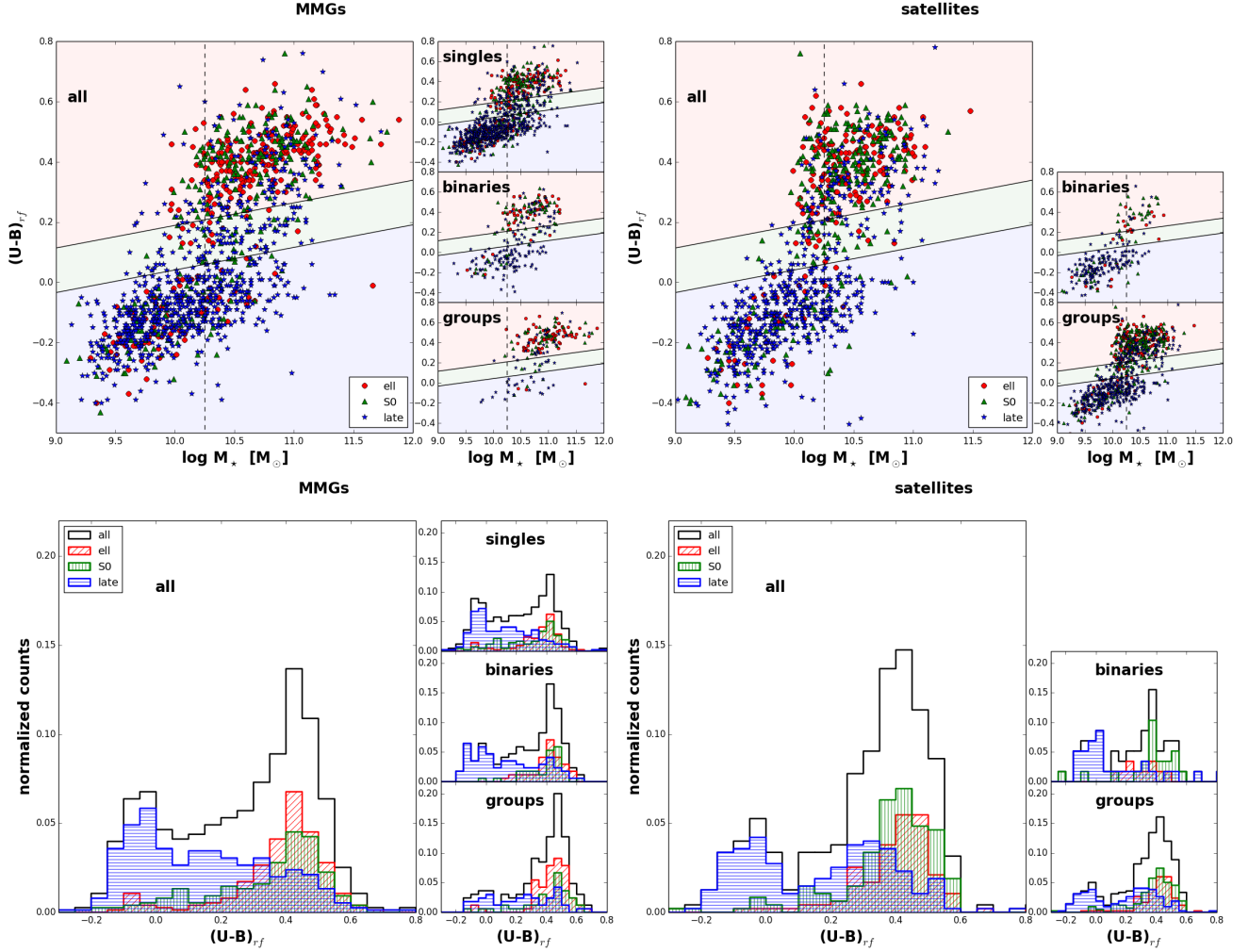


FIG. 2.— Rest frame $(U-B)_{rf}$ -mass relation (upper panels) and normalized rest frame $(U-B)_{rf}$ color distribution (bottom panels) for galaxies of different classes (left panels: MMGs, right panels: satellites) and morphologies in the different environments (shown in the smaller windows). Red circles and histograms: ellipticals; green triangles and histograms: S0s; blue stars and histograms: late types. In the upper panels, the black dashed vertical line represents the mass completeness limit, the black solid lines show the separation between red, green and blue galaxies (see text for details).

respectively. For both classes, this fraction decreases going from less to more massive environments. Ellipticals are instead found in the same proportion among MMGs and satellites. In addition, ellipticals and S0s are found in similar proportions among MMGs, while among satellites S0s are more frequent. These latter trends remain true when individual environments are inspected, except that ellipticals are more numerous than S0s in group MMGs. Thus, at odds with the color fractions, morphological fractions vary both between groups, binaries and singles and from MMGs to satellites in a given environment.

The bottom panels of Fig. 2 show that, even though a color bimodality exists for both MMGs and satellites, their color distributions are remarkably different: they both show a prominent red peak at $(U-B)_{rf} \sim 0.45$ and a secondary blue peak at $(U-B)_{rf} \sim -0.05$. Nonetheless, blue and green galaxies are more conspicuous among MMGs than among satellites, suggesting that only the blue fractions depend on environment and class. Going from the least toward the most massive environments, the two peaks of the distributions shift toward redder colors, the peak at blue colors gets less prominent while the number of galaxies with red color increases, indicating again that in groups galaxies are most likely red. This is valid for both MMGs and satellites.

Splitting galaxies by morphology, among MMGs, late types show an unimodal distribution with a long tail toward green and red colors, while among satellites they present a bimodal distribution, with a second peak almost as important as the first one, centered at quite red colors, and only a few green galaxies. Late types are the galaxies that show the most noticeable variation with the galaxy class and environment. Ellipticals and S0s are mostly red, but green and blue ellipticals and S0s are a non-negligible fraction. In MMGs, ellipticals and S0s show similar color distributions peaked around $(U-B)_{rf} \sim 0.4$. Both distributions show a tail of galaxies with blue colors. In satellites, instead, S0s are the most important population forming the red peak.

This analysis highlights the variation of the incidence of each sub-population with environment, and the well known fact that there is no one-to-one correspondence between color and morphology, i.e. not all late types have blue colors, and not all ellipticals and S0s are red.

In the following we refer to red late types, blue early-types and green galaxies of all types as candidate “transition objects”, because they are likely to have experienced, or being in the process of experiencing a transformation in color and/or morphology, from star-forming to passive, or viceversa.

Until now we have considered only galaxy colors and mor-

TABLE 1
PERCENTAGE OF GALAXIES OF DIFFERENT TYPES ABOVE THE STELLAR MASS COMPLETENESS LIMIT IN DIFFERENT ENVIRONMENTS.

	MOST MASSIVE GALAXIES						SATELLITES						
	ALL GALAXIES												
	COLOR			MORPHOLOGY			COLOR		MORPHOLOGY				
	<i>red</i>	<i>green</i>	<i>blue</i>	<i>ell</i>	<i>S0</i>	<i>late</i>	<i>red</i>	<i>green</i>	<i>blue</i>	<i>ell</i>	<i>S0</i>	<i>late</i>	
COLOR	<i>all</i>	60±3	14±2	26±2	28±2	25±2	47±3	72±3	9±2	19±3	25±3	35±3	40±3
	<i>red</i>				25±2	19±2	16±2				23±3	30±3	19±3
	<i>green</i>				1.2±0.6	3±1	9±2				1±1	3±1	5±1
	<i>blue</i>				2±1	3±1	21±2				1±1	2±1	16±2
	SINGLE GALAXIES												
	COLOR			MORPHOLOGY			COLOR		MORPHOLOGY				
	<i>red</i>	<i>green</i>	<i>blue</i>	<i>ell</i>	<i>S0</i>	<i>late</i>	<i>red</i>	<i>green</i>	<i>blue</i>	<i>ell</i>	<i>S0</i>	<i>late</i>	
COLOR	<i>all</i>	53±3	16±3	31±2	24±3	26±3	50±3		–	–	–	–	–
	<i>red</i>				20±3	17±3	16±2				–	–	–
	<i>green</i>				1±1	4±1	10±2				–	–	–
	<i>blue</i>				3±1	4±1	24±3				–	–	–
	BINARY SYSTEMS												
	COLOR			MORPHOLOGY			COLOR		MORPHOLOGY				
	<i>red</i>	<i>green</i>	<i>blue</i>	<i>ell</i>	<i>S0</i>	<i>late</i>	<i>red</i>	<i>green</i>	<i>blue</i>	<i>ell</i>	<i>S0</i>	<i>late</i>	
COLOR	<i>all</i>	59±5	14±4	27±5	26±5	21±5	53±6	57±9	12±6	31±9	17±8	36±9	47±9
	<i>red</i>				23±5	19±5	17±4				12±7	29±9	15±7
	<i>green</i>				2±2	0.5±0.1	11±4				5±5	2±2	5±5
	<i>blue</i>				0.6±0.1	1±1	25±5				0 ⁺¹ _{−0}	5±5	26±9
	GROUPS												
	COLOR			MORPHOLOGY			COLOR		MORPHOLOGY				
	<i>red</i>	<i>green</i>	<i>blue</i>	<i>ell</i>	<i>S0</i>	<i>late</i>	<i>red</i>	<i>green</i>	<i>blue</i>	<i>ell</i>	<i>S0</i>	<i>late</i>	
COLOR	<i>all</i>	79±5	7±3	14±4	42±6	26±5	32±5	74±3	9±2	17±3	26±3	34±3	40±3
	<i>red</i>				40±6	22±5	16±4				24±3	30±3	20±3
	<i>green</i>				0 ⁺¹ _{−0}	2±1	5±2				1±1	3±1	5±2
	<i>blue</i>				2±2	2±2	10±4				1±1	2±1	15±2

phologies, but these do not univocally distinguish between star-forming and passive galaxies. The red late-type sample might be contaminated by the presence of star-forming galaxies highly extinguished by dust³ and, viceversa, not all blue or green early types are necessarily forming stars. To isolate truly star-forming and truly passive galaxies, we inspect the level of SSFR ($=\text{SFR}/M_*$).⁴ From now on, we only consider red late-type objects with $\text{SSFR} < 10^{-12} \text{yr}^{-1}$ (RP late-type) and blue early-type objects with $\text{SSFR} > 10^{-12} \text{yr}^{-1}$ (BSF early-types).

4. TRENDS WITH MASS AND ENVIRONMENT

4.1. Mass trends in different environments

Calvi *et al.* (2012, 2013) have already shown that in the PM2GC galaxy morphology is linked with both stellar mass and environment. The mass distribution of each morphological type depends on the environment, and in each environment the mass function is different for ellipticals, S0s and late types. They found that there is little dependence of the morphological fractions on galaxy mass in the range $10.25 < M < 11.1$, while, at higher masses, this dependence is strong.

Here we take a complementary approach carefully inspecting also changes in color. At first, we apply only the cut in

color, for MMGs and satellites separately (Fig.3). Fractions strongly depend both on stellar mass and class. As shown in the left panels, the contribution of blue galaxies to the total population steadily decreases with mass. However, at any mass, blue galaxies are more numerous among MMGs than among satellites, being 40% of the entire MMG population at $\log M_*/M_\odot = 10.4$, and $< 25\%$ in satellites at the same mass. Also the fraction of green galaxies decreases with increasing mass, for both MMGs and satellites, though more gently than blue galaxies do. In contrast, the incidence of red galaxies increases with mass, and they dominate both galaxy classes at all masses.

Environmental variations of color fractions can also be observed comparing group and single MMGs: red/blue and green galaxies are less/more frequent among singles than in groups at a given mass. No significant differences are detected between group satellites and all satellites, as expected given the fact that 90% of our satellites are in groups. On the other hand, we note that considering only groups, color fractions as a function of mass are very similar for MMGs and satellites, indicating that differences between all MMGs and all satellites of a given mass are driven by the single MMGs.

More interesting than the simple green fraction is the number of green galaxies relative to the number of blue galaxies, which probably are evolutionary linked. Figure 4 presents the ratio of blue to green galaxies as a function of mass for all galaxies, for single and group galaxies and for MMGs and satellites. Trends are very similar in all cases, being the blue-to-green ratio always a factor 1:2 at high masses, 1:1 at intermediate masses, and 2.5-3:1 at lower masses. We will discuss the meaning of this ratio later, when we will discuss in detail the evolutionary links between green and blue galaxies.

³ We remind the reader that the Fritz *et al.* (2007) model includes a treatment of the dust, hence in principle our derived SSFRs already take into account the possible presence of dust and are corrected for that. In practice, models are not able to detect highly extinguished star formation in the optical without the aid of infrared data. The levels of SFR in our sample, however, are not expected to be extreme in the vast majority of cases thus our dust treatment and SFRs can be considered overall reliable.

⁴ The typical relative error on the SSFR is 35-40%.

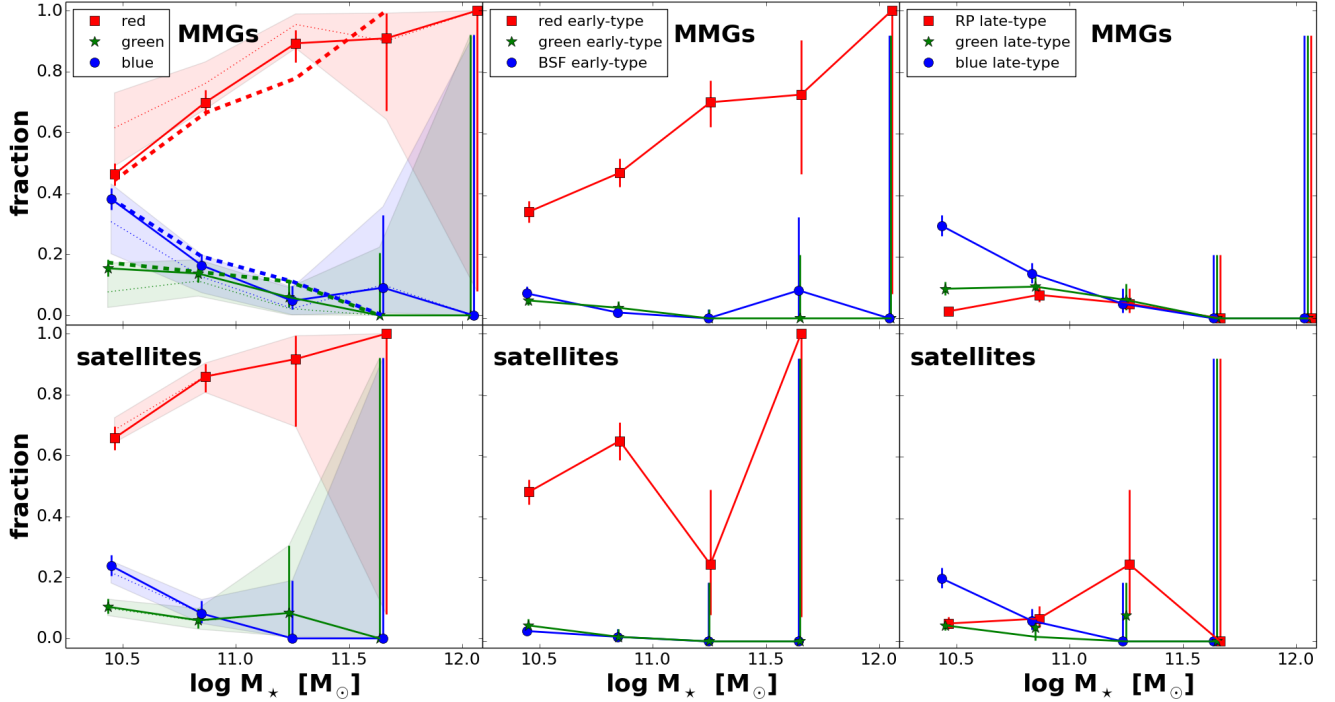


FIG. 3.— Fraction of galaxies as a function of stellar mass for MMGs (upper panels) and satellites (bottom panels). Left panels: color cut; red squares and solid lines: red galaxies, green stars and solid lines: green galaxies, blue circles and solid lines: blue galaxies. Dotted lines and shaded areas represent trends in groups, bold long dashes represent trends in single galaxies. Central panels: color+SSFR+morphological cut for early-type galaxies, as indicated in the labels. Right panels: color+SSFR+morphological cut for late-type galaxies, as indicated in the labels. Errors are defined as binomial errors (Gehrels 1986). Small horizontal shifts are applied to make the plot clearer.

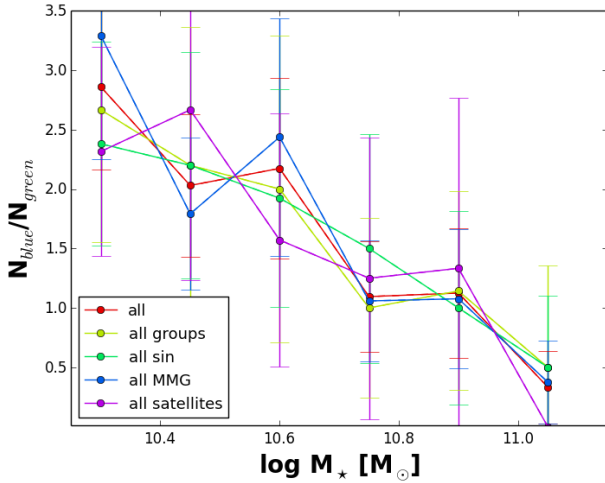


FIG. 4.— Ratio of the number of blue galaxies to the number of green galaxies as a function of stellar mass, for galaxies in different environments and of different class.

We now apply a joint subdivision in color, morphology and SSFR (central and right panels in Fig.3). Here and in the following figures, we consider together elliptical and S0 galaxies (early types), in order to increase the statistics and improve the readability of the panels.⁵ While the fraction of red early-types increases with mass,⁶ those of BSF and green early-types tend to decrease and are very close to zero at high

⁵ We note that for $\log M_*/M_\odot > 11$ ellipticals are twice as numerous as S0s (see also Calvi *et al.* 2012).

⁶ The observed dip in satellite red early types is probably due to galaxies with a consistent bulge but that have been classified as late types and small number statistics. Indeed, in Appendix A, where trends are inspected considering the Sérsic index instead of morphology, the fraction of red bulges steadily increases with mass.

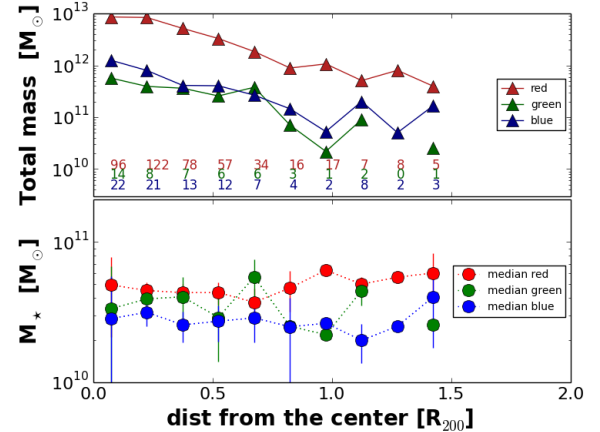


FIG. 5.— Total (upper panel), and median (bottom panel) stellar mass as a function of group-centric distance for red, green and blue MMG+satellite galaxies in groups above the mass completeness limit. Numbers are the number of objects in each bin.

masses. Also the trends for blue, green and RP late types are different, steadily declining the former, consistent with being flat with mass the others. This is true both for MMGs and for satellites. Moreover, RP late-type, BSF and green early-type trends with mass do not change with environment (groups vs. singles, plots not shown).

In §7 we will analyze in detail transition galaxies, but we first focus on trends in groups, where galaxy properties might be driven also by the location of the galaxies within the group.

4.2. Radial trends in groups

In groups there might be an additional parameter that can drive galaxy transformations, that is the position of galaxies within their structure. Indeed galaxies are expected to fall toward halo centers due to dynamical friction, therefore

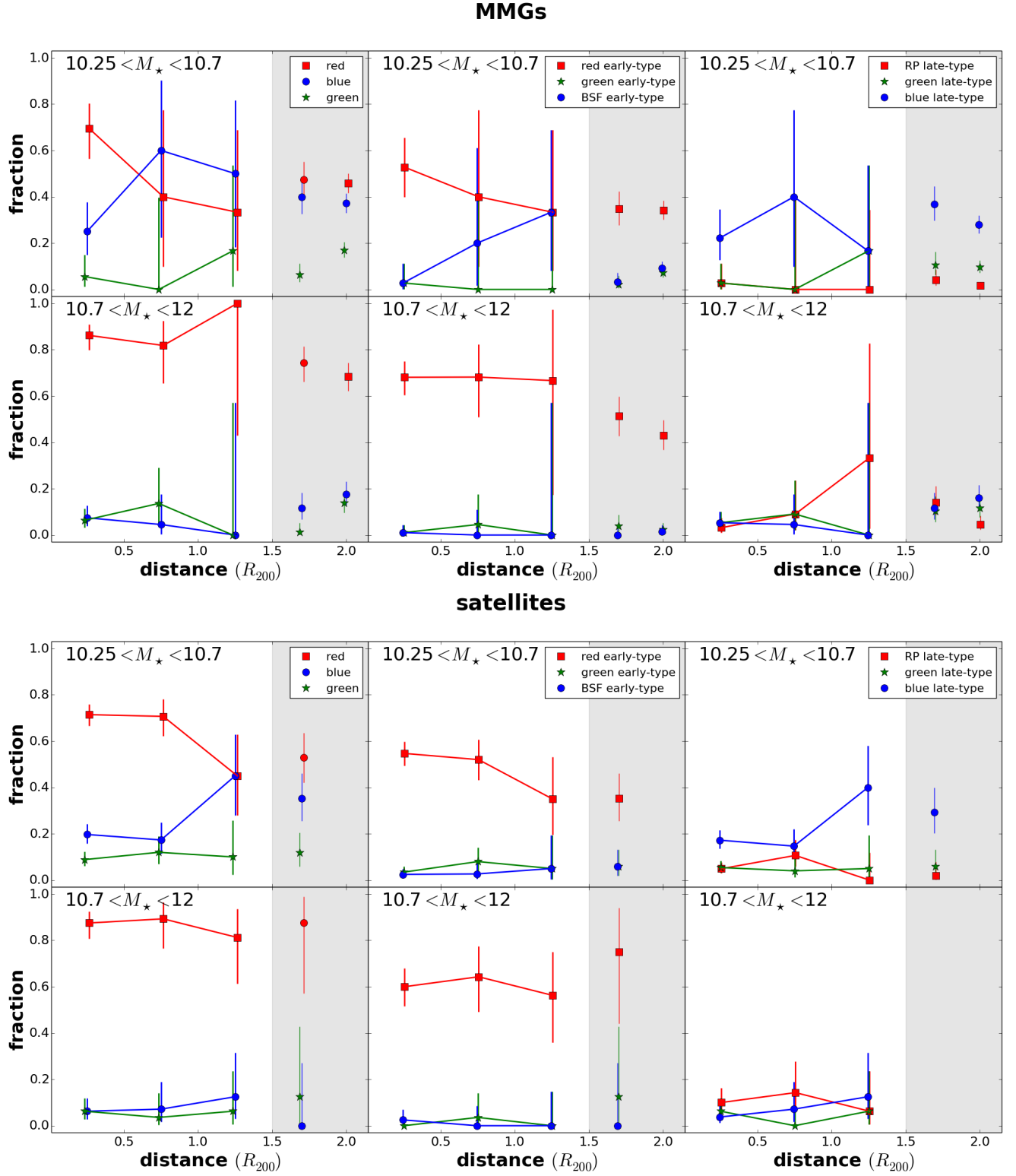


FIG. 6.— Fraction of galaxies as a function of group-centric distance in bins of stellar mass. Upper panels: MMGs, Lower panels: satellites. Left panels: all masses, central panels: $\log M_*/M_\odot < 10.7$, right panels: $\log M_*/M_\odot > 10.7$. Upper panels: color cut. Bottom panels: color+morphological cut. Colors and symbols are as in Fig. 3. Grey area represent galaxies that are not in groups, i.e. binary systems (placed at $r/R_{200}=1.7$) and single galaxies (placed at $r/R_{200}=2$). Small horizontal shifts are applied to make the plot clearer.

their group-centric distance is related to the time galaxies have spent inside the group (Weinmann, van den Bosch & Pasquali 2011; Smith *et al.* 2012; De Lucia *et al.* 2012).

We first look for signs of mass segregation with distance. Considering MMGs and satellites together, we sum the stellar mass of all galaxies (total mass). Figure 5 shows that, both for red, green and blue galaxies, the total mass in galaxies depends on group-centric distance: there is more mass close to the group center than in the outskirts, due to the larger number of galaxies at small group-centric distances. However, the median stellar mass is independent of distance, for galaxies of any color separately, as shown in the bottom panel. Fluctuations in trends of green galaxies are probably due to small number statistics: at $r > 0.7R_{200}$ there are only 7 galaxies. While green and blue galaxies present similar average masses, red galaxies are systematically more massive, of a factor of 2.

Therefore, stellar mass and position within a group are not strictly related and might play a different role in driving galaxy transformations. To separate the two contributions, we investigate how fractions depend on group-centric distance in bins of stellar mass.

We start analyzing galaxy color fractions in group and compare them to binary and single systems. Figure 6 show qualitatively similar trends for MMGs and satellites, though satellites have better statistics. At low masses (upper left panel), red galaxies dominate at small group-centric distances, while in the outskirts they are as common as blue galaxies, whose fraction increases with distance. The fraction of green galaxies is consistent within the errors with being constant with distance. At higher masses (lower left panel) all trends are flat, with red galaxies representing always ~ 75 -80% of the total population. In both mass bins, in binaries, galaxies of any color are, within the errors, about as common as galaxies of the same color in the group outskirts. The effect of environment is visible only among single galaxies for an excess of blue objects at high masses.

Considering also morphologies and star-forming properties, uncertainties increase, but some trends are still robustly detected. At low masses (upper central and right panels in Fig. 6), red early types dominate the populations, but their percentage slightly decreases with distance. In MMGs their decrease is mirrored by BSF early types, in satellites by blue late types. The fraction RP late types, green early types and late types is flat with distance. At higher masses, all trends are flat, with a possible excess of RP late types in the outskirts for MMGs. We do not detect any significant environmental variation.

4.3. Possible systematics

There are several possible biases or other effects in the data to consider in order to ensure the robustness of these results.

First of all, we note that any contamination of the group sample by field galaxies and vice versa, for which we are not applying any correction, will only render the observed trends less prominent. The real, corrected trends therefore would be even more pronounced.

As described in Calvi, Poggianti & Vulcani (2011), some of the groups are not fully contained in the narrow strip of the MGC survey and hence suffer from edge problems. 50 of these groups enter our sample, for a total of 313 galaxies. Removing them from our analysis, all the trends are recovered, within the errors (plots not shown). Since our results are not affected by these groups, we keep them in our sample to have a better statistics.

Our groups show a variety of galaxy richness: the smallest systems host only three members, the biggest one about 60 (Calvi, Poggianti & Vulcani 2011). As a consequence, results might be influenced by the different number of galaxies in groups, so we performed again our analysis splitting galaxies into two bins of richness: those in groups with $N_{gal} < 7$ members and those hosted in larger systems.⁷ This cut allows us to have almost equally numerous bins. No signs for a group-richness dependence are evident, except for the fact that richer groups tend to have more massive MMGs. All MMGs in the richest groups are more massive than $\log M_*/M_\odot = 10.7$ (plots not shown).

We also note that the uncertainty associated to the determination of the group centers might be quite large, especially for the groups composed by only 3 objects. Once again, the real, corrected, trends would be more noticeable.

In our analysis, we have distinguished between MMGs and satellites. However, MMGs do not always coincide with the galaxy closest to the group geometrical center. MMGs are mainly located in the central regions of the haloes (74% are within $r = 0.5R_{200}$), but not always at their very center (34% correspond also to the galaxy closest to the geometrical center).⁸ This can be understood as different stages in the hierarchical clustering process (Brough *et al.* 2008; Pimbblet 2008). We note that this fraction is in agreement with that estimated by Skibba *et al.* (2011), who computed the fraction of brightest non central galaxies as a function of the halo mass, finding it is 25% in low-mass haloes ($10^{12} h^{-1} M_\odot \leq M \leq 2 \times 10^{13} h^{-1} M_\odot$) and increases with halo mass. Our choice of contrasting MMGs and all other galaxies (common to many studies, e.g., Weinmann *et al.* 2006, 2009; Skibba, Sheth & Martino 2007; van den Bosch *et al.* 2008; Pasquali *et al.* 2009, 2010) most likely produces an underestimate of the true differences between centrals and satellites, hence trends might be even more pronounced.

5. OBJECTS IN TRANSITION

In the previous sections, we have investigated the color and morphological fractions as a function of stellar mass and environment. Such analysis has emphasized the presence of objects likely in transition from one type to the other. Above our mass completeness limit, $4 \pm 1\%$ of galaxies are BSF early types ($2 \pm 1\%$ of MMGs, $8 \pm 2\%$ of satellites), $4 \pm 1\%$ are green early types ($4 \pm 1\%$ of MMGs and $4 \pm 1\%$ of satellites), $8 \pm 1\%$ are green late types ($9 \pm 1\%$ of MMGs and $5 \pm 1\%$ of satellites), and $5 \pm 1\%$ are RP late types ($4 \pm 1\%$ of MMGs and $6 \pm 1\%$ of satellites).

We now analyze star formation levels, ages and structural parameters of these galaxies. From now on, we show the results for MMGs and satellites together, to increase the statistics, having checked that no substantial differences exist between the two populations, when the effect of the different mass distribution is considered.

Figure 7 presents the normalized distributions of the most relevant quantities for the objects in transition, compared to their normal counterparts: $M_{B_{Vega}}$ magnitudes, stellar masses, SFRs, SSFRs, Sérsic indexes, B/T ratios, (u-r) rest-frame color of bulges and disks, radii of bulges and disks. Figure 8 presents the same quantities as a function of stellar mass,

⁷ The cut is applied considering all members and not only those above the mass completeness limit.

⁸ In a few cases they are on the edge of the groups, though at least three MMGs at $r > 1R_{200}$ are found in groups that might suffer from edge problems.

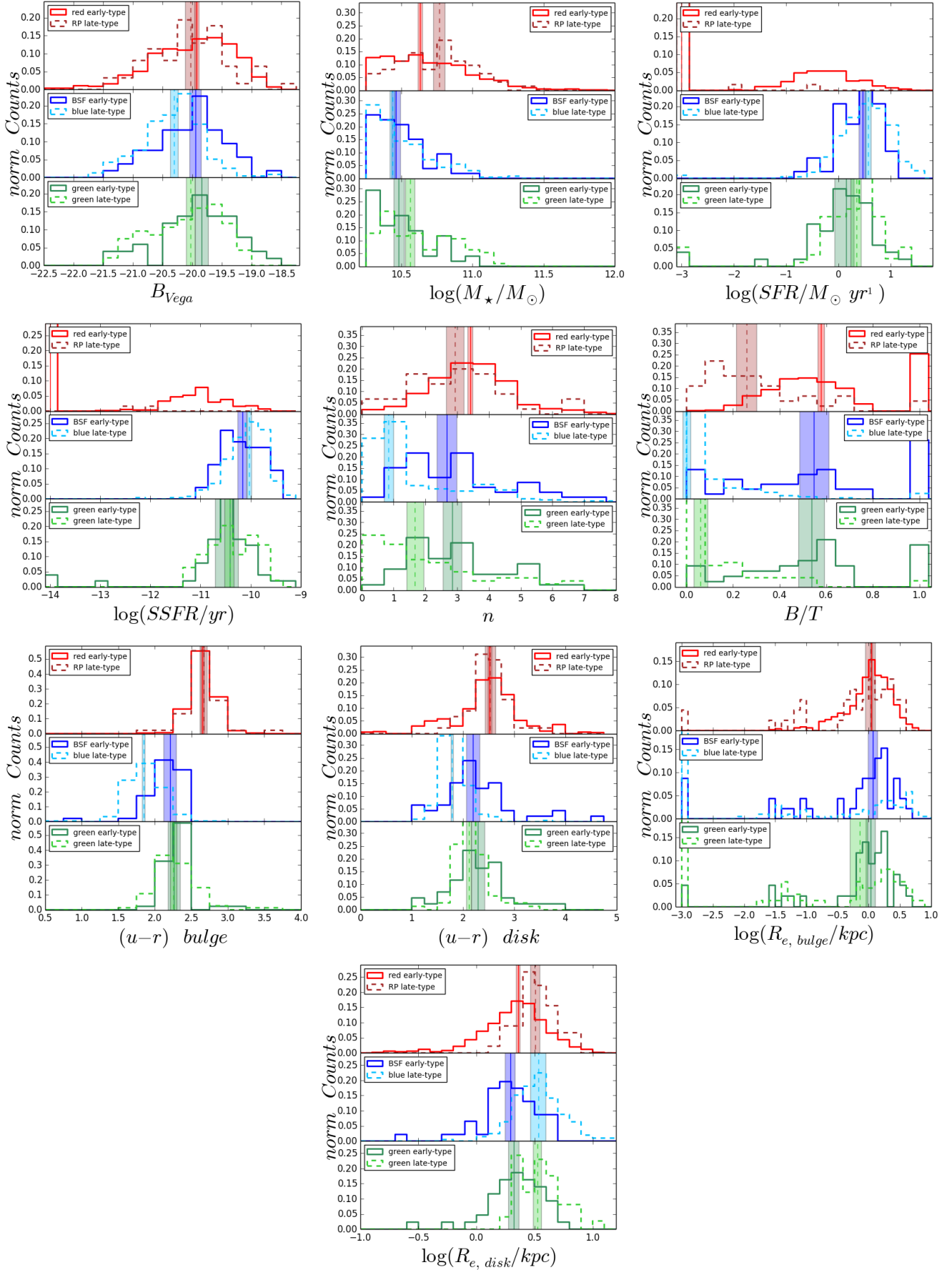


FIG. 7.— Normalized distributions for BSF early types (blue), green early types (dark green), red early types (red), blue late types (cyan), green late types (light green) and RP late types (dark red), as indicated in the labels. From top to bottom: B_{Vega} magnitudes, stellar masses, SFRs, SSFRs, Sérsic indexes, B/T ratios, $(u-r)_{rf}$ of bulges, $(u-r)_{rf}$ of disks, bulge effective radii, disk effective radii. Medians and errors on the medians are also shown.

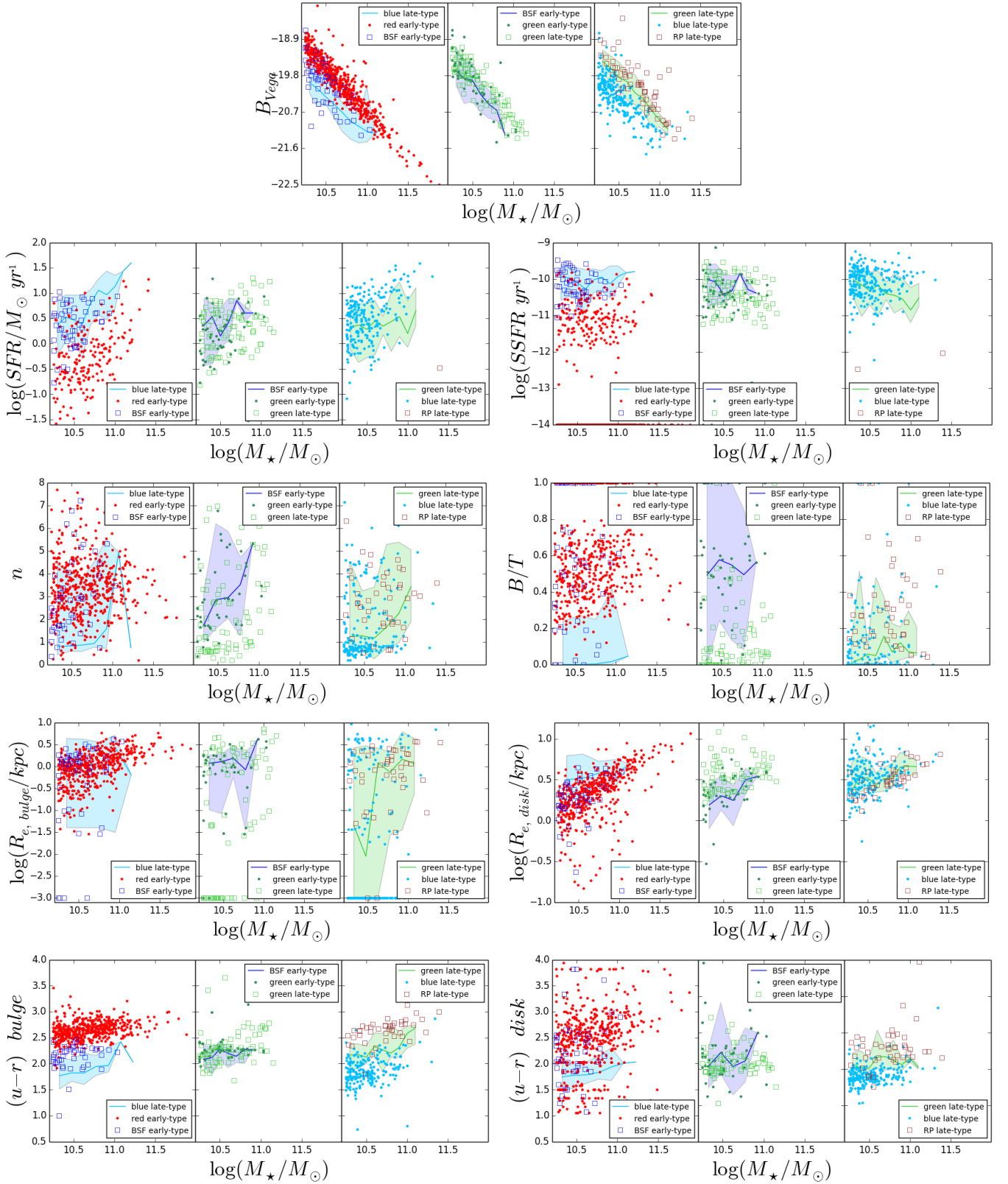


FIG. 8.— Properties as a function of mass for BSF early types (blue), green early types (dark green), red early types (red), blue late types (cyan), green late types (light green) and RP late types (dark red), as indicated in the labels. In each panel, three populations that might be evolutionarily linked are shown. For clarity, in each panel one population is represented by its median and a shaded area including its 10-th and 90-th percentiles. From top to bottom: B_{Vega} magnitudes, SFRs, SSFRs, Sérsic indexes, B/T ratios, $(u-r)_{rf}$ of bulges, $(u-r)_{rf}$ of disks, bulge effective radii, disk effective radii.

in order to show that the different mass distributions of the samples are not fully responsible for the differences observed in the stellar population and structural parameters. Table 2 gives the mean values of the aforementioned quantities, for all the different sub-populations. The quoted uncertainties on the median are estimated as $1.253\sigma/\sqrt{N}$, where σ is the standard deviation about the median and N is the number of galaxies in the sample under consideration (Rider 1960).

In the following, we directly compare the properties of the objects in transition to those of the subpopulations that might share a similar history with them.

5.1. Blue star-forming early types

We now compare BSF early types to red early types and blue late types (Fig. 7 and left panels of Fig. 8). Since ellipticals and S0s are expected to be characterized by different properties, in Appendix B we report the differences between these two populations.

The mass distribution of BSF early types is very similar to blue late types, while red early types are systematically more massive. At any given mass, BSF early types are on average brighter than their red counterparts, but fainter than blue late types.

The SFR-mass (and SSFR-mass) relations are similar for BSF early types and blue late types, but that of BSF early types is truncated at $\text{SFR} \sim 10 M_\odot$, while that of blue late types is not. In contrast, the SFR-mass relation for the subset of red early types that are star-forming is well below the standard relation at all masses.

BSF early types resemble their red counterparts in the n -mass plane. They span the whole range of B/T ratio, from pure disks to pure bulges. Both their n and B/T distributions are very different from those of blue late types.

The bulge and disk colors of BSF early types are in between those of their red counterparts and blue late types. Bulges lie on the upper edge of the corresponding blue late types color-mass relation, while most of the disks lie just above it. In addition, while most of the bulges follow the same mass-size relation in BSF and in red early types, we detect a subpopulation that is more than an order of magnitude smaller. This bimodality in bulge size is seen also in the BSF late-type population, where many galaxies have no bulge. Disks in BSF galaxies have similar sizes to those in red galaxies and trace the lower edge of the blue late-type relation.

We also analyzed the concentration of light (as derived in Abraham *et al.* 1994), mass and luminosity weighted ages⁹ and the fractions of mass enclosed in the bulge (plots not shown). BSF are less concentrated and systematically younger than red early types. In addition, BSF and red early types of similar mass have a quite similar fraction of mass in the disk, but a few BSF galaxies host a higher fraction of mass in the disk than their red counterparts.

5.2. Green early types

Figure 9 shows the morphological distribution of green galaxies and blue and RP late types. Focusing on the first population, it emerges it is mainly composed of late types but includes also some ellipticals and S0s. In Appendix B we will discuss in details the differences between these two populations, here we just focus on all early types.

⁹ Following the definition of Cid Fernandes *et al.* (2005), the luminosity-weighted (mass-weighted) age is computed by weighting the age of each SSP composing the integrated spectrum with its bolometric flux (mass).

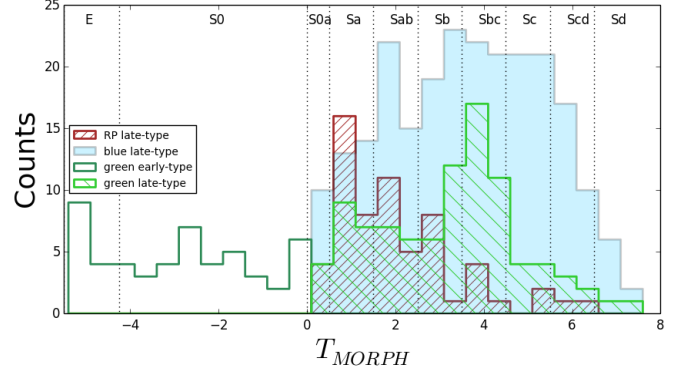


FIG. 9.— Finer morphological distribution of all (MMG+satellites) green, RP late types and blue late types, above the mass completeness limit.

The properties of green early types can be compared to those of green late types and BSF early types (Fig. 7 and central panels of Fig. 8). Green early types and BSF early types have similar mass distributions and maximum mass ($\log M_*/M_\odot \sim 11.1$), while green late types are slightly more massive. Green early types and BSF early types have similar Sérsic indexes, B/T ratios, similar color in the bulge and the disk, similar sizes of bulge and disks. At any fixed stellar mass, they only show a light reduction of star formation (SFR and SSFR).

5.3. Green and red passive late types

We now compare green, RP and blue galaxies with a late-type morphology. Fig. 9 shows that the RP morphological distribution is clearly skewed to earlier types compared to that of blue late types, but intermediate and late-type spirals are present too. Green galaxies show an intermediate distribution between the two.

Also the mass distribution of green galaxies is intermediate between that of blue (less massive on average) and RP (more massive), even though the maximum mass reached is similar in the three samples (Fig. 7).

In addition, most green late types are not completely quenched yet: their SSFR distribution indicates that most of them are still forming stars, only at a lower average rate than blue galaxies of similar mass. Only a few ($\sim 5\%$) green late types are already completely passive. The colors of both their bulges and disks are intermediate between red and blue, indicating that both of these structures are experiencing reduced levels of star formation (Fig. 7 and right panels of Fig. 8).

As for their structure, green late types are characterized by somewhat more prominent bulges than blue late types: on average, they have slightly larger Sérsic indexes, slightly higher B/T ratios, larger bulges than blue galaxies of similar mass.

Focusing on RPs, almost all the distributions point to differences with blue galaxies: RP late-type galaxies are on average fainter in the B-band, much more massive, have higher n and B/T, much redder bulges and disks, quite similar bulge and disk sizes but with the tendency to be on the smaller/more compact side of the size-mass distributions than blue late-type galaxies of similar mass.

In addition, at a given stellar mass, RP late types are also noticeably older and contain a higher fraction of mass in the bulge than blue late types (plots not shown).

5.4. Post-starburst galaxies

Another way to understand how blue, star-forming galaxies turn into red, passive systems is to directly look at their spec-

TABLE 2
CHARACTERISTIC NUMBERS OF OBJECTS IN TRANSITION, COMPARED TO NORMAL GALAXIES OF THE SAME MORPHOLOGY.

Quantity	red		green		blue	
	early-type	passive late-type	early-type	late-type	SF early-type	late-type
number	576	62	51	94	50	236
$\langle B_{Vega} \rangle$	-19.93 ± 0.04	-20.0 ± 0.1	-19.84 ± 0.1	-20.03 ± 0.07	-19.9 ± 0.1	-20.31 ± 0.06
$\langle \log M_*/M_\odot \rangle$	10.63 ± 0.04	10.76 ± 0.05	10.48 ± 0.05	10.56 ± 0.05	10.46 ± 0.05	10.43 ± 0.03
$\langle SFR \rangle (M_\odot \text{yr}^{-1})$	0 ± 0	0 ± 0	1.4 ± 0.5	2.2 ± 0.5	2.9 ± 0.5	3.6 ± 0.5
$\langle SSFR \rangle^\alpha (yr^{-1})$	$(9 \pm 3) 10^{-12}$	$(6 \pm 3) 10^{-13}$	$(4 \pm 2) 10^{-11}$	$(4.2 \pm 0.8) 10^{-11}$	$(6 \pm 1) 10^{-11}$	$(9.4 \pm 0.9) 10^{-11}$
$\langle n \rangle$	3.41 ± 0.08	2.9 ± 0.3	2.8 ± 0.3	1.7 ± 0.2	2.7 ± 0.3	0.8 ± 0.1
$\langle B/T \rangle$	0.58 ± 0.01	0.26 ± 0.04	0.54 ± 0.06	0.06 ± 0.03	0.55 ± 0.06	0 ± 0
$\langle R_e (bulge) \rangle (kpc)$	1.10 ± 0.05	1.07 ± 0.2	1.1 ± 0.2	0.7 ± 0.2	1.2 ± 0.2	0 ± 0
$\langle R_e (disk) \rangle (kpc)$	2.28 ± 0.09	3.2 ± 0.3	2.1 ± 0.2	3.3 ± 0.3	2.0 ± 0.2	3.4 ± 0.5
$\langle (u-r) bulge \rangle^\beta$	2.65 ± 0.02	2.67 ± 0.05	2.26 ± 0.09	2.26 ± 0.05	2.21 ± 0.09	1.84 ± 0.22
$\langle (u-r) disk \rangle^\beta$	2.52 ± 0.04	2.5 ± 0.1	2.3 ± 0.1	2.11 ± 0.05	2.2 ± 0.1	1.79 ± 0.02

$^\alpha$ Values computed only with galaxies with $SSFR \neq 0$

$^\beta$ Colors are in the AB system

tra, and seek for signs of such transition. Adopting the spectral classification defined by Dressler *et al.* (1999, MORPHS collaboration), we identify $k+a$ galaxies, whose spectra display a combination of signatures typical of both K and A-type stars with strong $H\delta$ in absorption and no emission lines. These features are typical of so called post-starburst/post-starforming galaxies whose star formation was recently (at some point during the last 0.5-1 Gyr) truncated over a short timescale, typically shorter than a few times 10^8 yr.

In our mass limited sample, 4.5% of all galaxies can be classified as $k+a$. This fraction is independent of environment. However, when considering the relative number of $k+a$ and blue galaxies, this is much higher in groups ($22 \pm 6\%$) than in binaries and singles ($13 \pm 5\%$), suggesting a higher efficiency of sudden quenching in groups compared to lower mass haloes.

In our sample, 32 $k+a$ are red (8 RP late types), 13 are green and 10 are blue (1 BSF early-type). This shows that the majority of those galaxies that are truncated on a short timescale cannot be recognized based on color or color+morphology, but only performing a detailed spectral analysis. The $k+a$ channel is therefore another transition channel that needs to be considered to build a complete picture of galaxy transformations, that affects 4.5% of all galaxies on a timescale of ~ 1 Gyr.

Finally, we note that only 6% green early types and 10% of green late types are $k+a$, confirming that most of the green galaxies are due to a SF decline on a longer timescale.

5.5. SFHs of the different populations

We now investigate the SFHs of the different galaxy populations. To reduce the effect of the stellar mass in quenching galaxies, we consider two different mass bins: $10.25 < \log M_*/M_\odot < 10.7$ and $10.7 < \log M_*/M_\odot < 11.15$. We do not include more massive galaxies due to the lack of statistics. We verified that no significant residual dependence on mass distribution remains in each mass bin.

We compute the mean SFR per galaxy in 5 age intervals ($t=0.877, 4.079, 9.021, 11.863, 12.345$ Gyr) and compare the trends for galaxies of different colors and/or star-forming properties. Errors on mean values are obtained using a bootstrap resampling. Figure 10 shows that galaxies with different properties today are characterized by different average SFHs, which also depend on stellar masses.

Blue late types are currently forming stars,¹⁰ and the slope

of their decline in star formation with time depends on stellar mass, being steeper for more massive galaxies. In both mass bins green late-type galaxies have the same SFH of blue late types at early epochs, the only difference being a significant turn-down of their star formation in the last 1-3 Gyrs (last one or two time bins depending on mass). This is consistent with green late types being regular blue late types until a few Gyr ago, when they experienced a reduction (not yet a complete halting in most cases) of the star formation activity. Green early- and late types show very similar SFHs (plot not shown).

Except for the first bin at high masses, BSF early types have SFHs identical to blue late types. This is consistent with BSF early types being blue late types that suffered an alteration of their morphology. The average SFH of red early types with $SSFR < 10^{-12} \text{yr}^{-1}$ is instead very different from that of BSF early types, and of all other subsamples: these galaxies were forming stars at a high rate at early epochs, then their SFR declined steeply with time. This effectively rules out the RP early types as candidate progenitors for the BSF early types.

Moving the attention to RP late types, their SFH strongly depends on stellar mass (being steeper at higher masses) and does not resemble that of blue late types, showing a much stronger variation with time. In the last ~ 6 Gyr their average SFR is lower than that of blue late types of similar mass. Most probably, the RP late-type population comprises all late-type galaxies that have stopped forming stars at any epoch and that have retained their morphology. Indeed, inspecting the SFH of individual galaxies, we find a number of RP late types that have stopped forming stars at intermediate or even high redshifts, $\sim 30\%$ at $z \geq 0.3$. Therefore, it is quite logical to expect an average star formation decline as the one observed: those late types that stopped forming stars at an early epoch only contribute in this plot in the oldest age bins, making the decline slope steeper. In this sense, it is not logical to search for an evolutionary direct connection between all of today's RP late types and today's blue late types: only the subset of latest arrivals of the former have recently evolved from the latter. The differences in the right panel of Fig.10 can be explained in such a scenario.

6. COLOR EVOLUTION FOR DIFFERENT QUENCHING HISTORIES

To investigate what type of star formation history can produce a green galaxy spectrum, and for how long, we employ our spectrophotometric model described in §2 (Fritz *et al.* 2007, 2011) to compute the color of galaxies with different

and their influence is negligible.

¹⁰ Blue late types with $SSFR < 10^{-12} \text{yr}^{-1}$ are 2% of all blue late types,

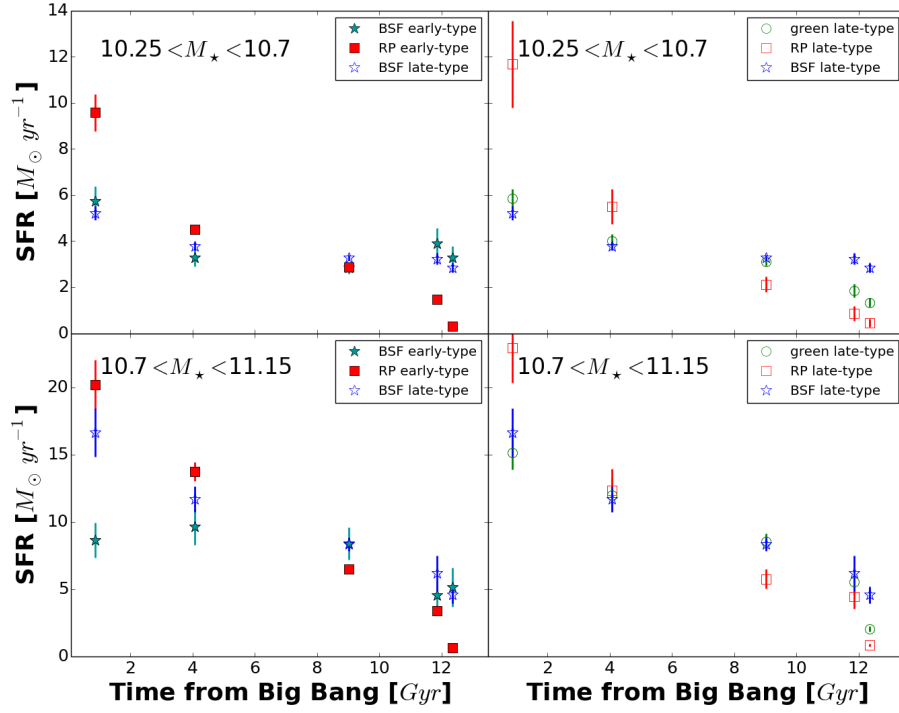


FIG. 10.— Mean SFR as a function of cosmic time for galaxies of different colors and/or star-forming properties, as described in the labels. Top panels: galaxies with $\log M_*/M_\odot < 10.7$. Bottom panels: galaxies with $10.7 < \log M_*/M_\odot < 11.15$. Errors on mean values are obtained using a bootstrap resampling.

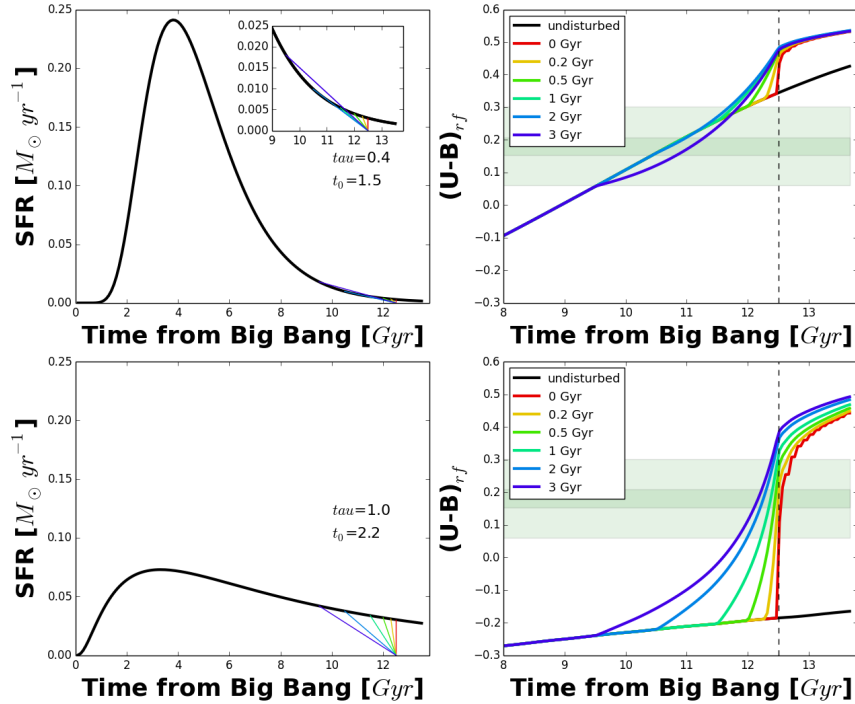


FIG. 11.— Color of galaxies with different histories and different quenching timescales according to the spectrophotometric model of Fritz *et al.* (2007, 2011). Left panels: SFRs as a function of time with different τ and t_0 , as written in the labels. The linear decline with different timescales is also shown with different colors. In the upper panel, a zoom of the decline is also shown. Right panels: $(U-B)_{rf}$ color as a function of time for the SFRs shown in the left panels. The different declines are also shown. Green shaded areas show our definition of green galaxies (see §3) for galaxies with $\log M_*/M_\odot < 10.25$ and $\log M_*/M_\odot < 11.5$.

histories and different quenching timescales. We use the SFH lognormal analytic form of Gladders *et al.* (2013):

$$SFR(t, t_0, \tau) = \frac{1}{t\sqrt{2\pi\tau^2}} \exp - \frac{[\ln(t - t_0)]^2}{2\tau^2} \quad (4)$$

where t is the elapsed time since the Big Bang, t_0 is the logarithmic delay time, and τ sets the rise and decay timescale. This form has been shown to be a good representation of galaxy SFHs.

We consider galaxies with various lognormal parameters (t_0 and τ) and compute their $(U - B)$ rest-frame color assuming: a) no quenching at any time; b) a sudden quenching, i.e. an abrupt interruption of the star formation activity on a timescale $t_{\text{quench}} = 0$; c) a linear decline of the SFR from the undisturbed level to zero with short to long timescales: $t_{\text{quench}} = 0.2, 0.5, 1, 2, 3$ Gyr. By construction, all the histories have a SFR equal to 0 1.1 Gyr ago.

Figure 11 illustrates two emblematic cases of our modeling: one with a short τ (usually considered typical of early spirals) and one with a long τ (typical of late spirals). In the first case, galaxies can assume green colors for ~ 2.5 Gyr even without being subject to a quenching event, while in the second case intermediate colors are probably a sign of quenching. A short quenching time ($t_{\text{quench}} = 0 - 0.5$ Gyr) produces a very short green phase (~ 0.15 Gyr), that might be hardly observable, while galaxies whose SFR declines with $t_{\text{quench}} = 1 - 3$ Gyr go through a green phase that lasts for 0.25-0.5 Gyr.

Galaxies with a very short τ (~ 0.3 , typical of early types) do not go through a green phase at least in the last 6 Gyr (plot not shown).

To conclude, our modeling shows that green colors are due to SFHs declining with long timescales. These could be due either to “undisturbed” lognormal histories with short τ s, or to long τ galaxies that are quenched on the timescales of the order of 1 Gyr or more. Green colors are therefore not necessarily indicative of “quenching” processes.

7. DISCUSSION

In this paper we have investigated how galaxies of different stellar mass transform from one type to another in a variety of environments (groups, binary systems, single galaxies), in the local universe. We found that a non negligible fraction of objects is likely in a transitional phase, that is they are experiencing or have recently experienced a transformation from being star-forming to passive, or viceversa. We have seen that there is not a one-to-one correspondence between color and morphology, and confirmed that in many cases these two quantities must change on different timescales and might have a different dependence on stellar mass, environment and galaxy class. We have then investigated the properties of the galaxies in transition, and compared them to those of their “normal” counterparts, to understand whether also their structural properties are different, or whether variations are limited to the efficiency of the SFR, which is mainly reflected in the galaxy color. Finally, we inspected SFHs, to gain insights of the rate at which all galaxies have been forming stars in the past.

7.1. A possible evolutionary scenario

We are now in the position of proposing a possible evolutionary scenario for galaxies, as summarized in Figure 12.

From blue late types...

We start considering blue (star-forming) late-type galaxies. At a certain epoch, because of secular and/or environmental

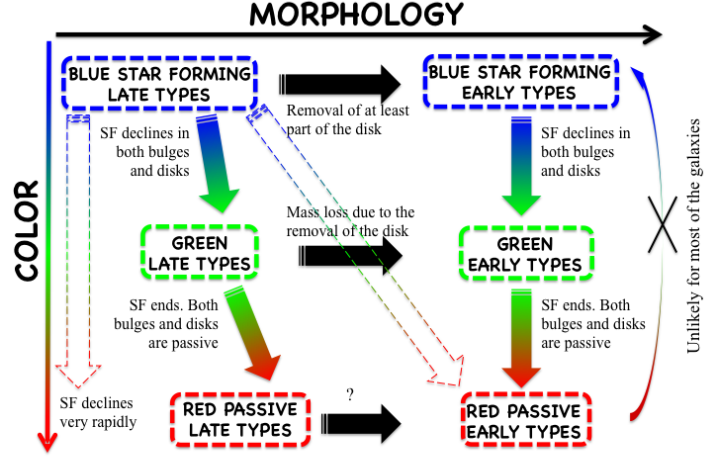


FIG. 12.— Illustration of our main results and interpretation.

processes, their gas supply is affected and their SFR starts to decline, either on a short or a long timescale. Therefore, a change in color must occur, either accompanied by a change in morphology or not. Various scenarios are possible at this stage.

...to green late types

If the SFR declines, blue late types can turn into green late types. Indeed, these two families share a similar SFH for most of the time, with green late types showing a reduction of the SFR only in the last few Gyr (Fig.10). Therefore, green late types are most probably the result of blue late types that have their SFR suppressed, but not yet extinguished, both in the bulge and in the disk. The analysis of their structural parameters is consistent with this picture, if a small structural variation takes place, in the sense of a small increase of the bulge relevance from blue to green. According to our modeling, galaxies can assume green colors for ~ 2.5 Gyr if their SFR is characterized by short τ even without being subject to any quenching event. Alternatively, galaxies whose SFR is characterized by long τ can remain green for up to 1 Gyr as a consequence of a quenching event.

... or to BSF early types

If the morphology changes before star formation is shut off, blue late types can turn into BSF early types. The analysis of the SFHs, and their mass distributions support this hypothesis. Structural parameters of blue late types and BSF early types show significant differences instead, as expected if a morphological transformation has occurred. At any given mass, the disk in BSF early types is not only smaller and fainter (different B/T ratio distribution) but also less massive, suggesting that the morphological transformation happened with a removal of at least part of the stellar disk.

From green late types...

Subsequently, green late types can further undergo to a change in color, and turn into RP late types, or change their morphology and become green early types.

... to RP late types

If no major morphological transformation occurs,¹¹ green late types most likely become RP late types. Compared to their first progenitors (blue late types) and their possible recent progenitors (green late types), RP late types are systematically more massive, and at a given stellar mass have a smaller disk. These results, together with the analysis of SFHs, suggest that RP late types today can not derive only from the current blue and green late types via the quenching and fading of a disk. They are probably an heterogeneous population which comprises all late type galaxies that have stopped forming stars at any epoch and that retained their morphology. The non negligible fraction of post-starburst galaxies ($\sim 15\%$) in RP late types suggests that some of these objects became red after a very short (therefore virtually unobservable) green phase.

... or to green early types

If green late types are subject to a morphological transformation, they might become green early types. The analysis of the SFH supports such possibility, since no differences in SFH have been detected between the two populations (plot not shown). Green early types are characterized by a steeper mass distribution than the green late types, which extends toward slightly higher masses. The analysis of the structural parameters suggests that this mass loss is mainly related to the progressive disappearance of the disk, which at any given stellar mass is smaller and less massive. The properties of the bulges of green late types and green early types are more similar, as a consequence the relative proportion of bulges and disk changes, as reflected in the distribution of B/T ratios.

From BSF early types to green early types

Green early types can also derive from BSF early types which suffer a reduction of their SFR and a consequent change in color. Indeed, green and BSF early types present very similar mass and structural parameters (Sérsic indexes, B/T ratios, size of bulges and disks) distributions, supporting this scenario.

From green early types and RP late types to red early types

Finally, both green early types and RP late types can eventually turn into red early types. However, given the fact that the RP early-type population contains galaxies that stopped forming stars at any earlier epoch, which were characterized by different structural properties, comparisons between such populations are very hard and it is difficult to state the frequency of such transformations.

In principle, red early types might suffer a rejuvenation process that makes them change colors. Indeed, some structural parameters of red and BSF early types are similar, consistently with the hypothesis a common origin. However, this scenario seems to be ruled out by the characterization of the SFHs which are clearly different for the two populations.

Adopting a different galaxy selection, Tojeiro *et al.* (2013) found that red late-type spirals are recent descendants of blue late-type spirals, sharing similar SFHs at early times and showing a reduction of the star formation only in the last 500 Myr. On the basis of the SFH and dust content, they claimed

red early-type spirals are more likely to evolve directly into red ellipticals than red late-type spirals. They also found that blue ellipticals show similar SFHs as blue spirals, except for a reduction of the efficiency of the star formation in the last 100 Myr. Blue ellipticals have different dust content than all spiral galaxies, ruling out the scenario according to which most of them derive from blue spirals.

7.2. The physical processes responsible for galaxy transformations

Different mechanisms have to be at work to produce the observed transformations.

Color transformations are due to a reduction and suppression of the SFR both in bulges and disks. They can occur as the result of an external process or simply because galaxies use up all of their gas and shut down their star formation while they retain their structure.

In the case of late types, by taking a realistic accretion histories from cosmological simulations, Forbes, Krumholz & Burkert (2012) have shown that a certain fraction of disks in the course of their lifetimes is expected to experience a period of low accretion during which they will exhaust their gas supply and become redder, only to return to the blue cloud with the resumption of higher accretion rates.

Ram pressure stripping of cold gas (Gunn & Gott 1972; Feldmann, Carollo & Mayer 2011), and strangulation of the galactic system by removal of hot and warm gas necessary to fuel star formation (Larson, Tinsley & Caldwell 1980; Balogh, Navarro & Morris 2000; Font *et al.* 2008) might be responsible for such transformations, since they are expected not to affect galaxy morphology, at least not directly. However, we do not detect any environmental dependence (see §7.3), suggesting these processes are not very efficient. In addition, while ram pressure is observed to act on galaxies in high-mass clusters, it has not been observed in lower mass groups, where lower halo gas densities and satellite velocities likely lower its efficiency. Moreover, haloes of $M_* \sim 10^{12} M_\odot$ are not expected to have virial shock fronts which support hot, virialized gas within the halo (Dekel & Birnboim 2006), so in this mass regime it is not clear that either strangulation or ram pressure can be efficient. This may suggest tidal stripping (e.g., Park, Gott & Choi 2007 and references therein), or harassment and/or mergers induce rapid cold gas consumption that quenches star formation. However, all these processes are also responsible for a morphological variation, since the distribution of the light and gas are also affected. Since the external parts of the galaxies first feel these processes, it is plausible that they first affect disks, producing their observed fading. Therefore, a morphological change in the direction of an increase of the B/T ratio might actually be an aftermath of quenching, simply due to the fading and the reduction of a star-forming disk once star-formation is reduced or ceased.

7.3. Lack of environmental effects

Our analysis has revealed very little evidence for environmental effects on galaxy transformations.

The relative proportion of green and blue galaxies has been found to be almost constant with environment (groups, binaries, satellites, and as a function of group-centric radius) and also for MMGs and satellites, implying that changes in color occur on a time scale that does not depend on host halo mass, halo-centric radius or on being a central or a satellite in a halo. In alternative, if most green galaxies are not due to quenching, the constancy of the green to blue ratio would indicate

¹¹ A minor morphological transformation from late spirals to slightly earlier spirals is favored by the morphological distributions of green late types vs. blue late types.

that the processes giving origin to long and short τ SFHs do not change efficiency with environment. The decline in star formation giving rise to green galaxies is therefore not due to environmental effects. On the other hand, the relative fraction of green and blue galaxies depends on mass, being a factor 2:1 at high masses, 1:1 at intermediate masses, and $\sim 1:3$ at lower masses, suggesting that the decline in star formation in green galaxies is related to galaxy mass.

The only detected environmental effects are that 1) in single-MMGs, at any given mass, there are proportionally more blue and green galaxies than in the other environments, and in general they are proportionally less massive and 2) in groups there might be a higher fast quenching efficiency which gives origin to post-starburst signatures.

Our findings might be quite surprising, given that a host halo's virial radius broadly corresponds to a physical transition from the low-density field environment to a high-density region where dark matter and gas are virialized, therefore environmental effects would be expected.

On the other hand, it is important to keep in mind that environmental dependences can extend to galaxies beyond the virial radius of a group/cluster (as largely discussed in Wetzel *et al.* 2014). Therefore the (lack of) trends are plausibly driven, at least in part, by those galaxies having passed within much smaller distances from a group/cluster, but at the time of the observations are found very far from it. Also a large fraction of central galaxies near massive host haloes are actually ejected satellites (e.g., Wetzel *et al.* 2014). Balogh, Navarro & Morris (2000) first noted from N-body simulations of clusters that particles that have passed within the virial radius can then orbit well outside of it. 'ejected' (or 'backsplash') satellites (see e.g. Gill, Knebe & Gibson 2005; Bahé *et al.* 2013) typically orbit back out to a maximum distance of $\sim 2.5 R_{200}$ beyond a host halo after passing through it. In addition, almost half of all galaxies within this distance are composed of these ejected satellites, which are preferentially quiescent (e.g. Wang, Mo & Jing 2009; Wetzel *et al.* 2013), with higher fractions for less massive galaxies and around more massive host haloes. Thus, ejected satellites are potentially critical for understanding the properties of galaxies near groups/clusters and obtaining a complete picture of environmental dependence.

7.4. The importance of the galaxy structure

Recently, the importance of galaxy structure for galaxy transformations has been widely discussed in the literature.

Carollo *et al.* (2014) report that the quenched satellites at low z have larger B/T and smaller half-light radii than the star-forming satellites. They find that differences are mostly due to differences in the disks, which have lower luminosities in the quenched galaxies, but they can not be explained by uniformly fading the disks following quenching. Instead, either there must be a differential fading of the disks with galaxy radius or disks were generally smaller in the past, both of which would be expected in an inside-out disk growth scenario.

Other literature results focused mainly on the bulge, finding that its properties might play a role in quenching galaxies, rather than the disk. For example, in the local universe, Abramson *et al.* (2014) showed that the increase in bulge mass-fractions, which are portions of a galaxy not forming stars, is responsible for the existing anti-correlation between $SSFR$ and M_* . At $z < 0.2$, the passive fraction for central galaxies has been found to be closely correlated to the bulge mass (Bluck *et al.* 2014) and to the B/T ratio (Omand,

Balogh & Poggianti 2014). At $0.5 < z < 2.5$ Lang *et al.* (2014) found an increased bulge prominence among quiescent galaxies, with an increase of the typical B/T among star-forming galaxies above $10^{11} M_\odot$. These findings have lead some authors to suggest that the physical mechanisms responsible for the quenching of star formation must be strongly coupled to the formation or accretion of the bulge.

Our analysis confirms that the relative importance of the bulge and the disk appears to be a key parameter in galaxy transformations. We found that a *morphological* transition (from BSF late types to BSF early types, from green late types to green early types) is mainly due to the fading and total or partial removal of the disk. A transition in star formation with no morphological change, instead (from blue late types to green late types) is accompanied by a small structural change: as we have seen in §5.3, the average B/T ratio and mass ratio of bulge and disk in green late types is only slightly higher than in blue late types. In this case the differences in these ratios can be ascribed to bulge growth instead of disk fading, but the effect is overall small on the population.

7.5. Quenching times

According to our modeling, galaxies which sustain a green color for a non-negligible interval of time (> 0.5 Gyr) can originate either from a long timescale (> 1 Gyr) quenching of long τ galaxies, or from short τ "undisturbed" star formation histories typical of intermediate types. Galaxies with a short quenching (0-0.5 Gyr) timescale do exist, but they sustain green colors for a short period of time and they are observable as $k+a$ galaxies that quickly transit from being blue to being red.

We have shown that the occurrence of green galaxies (compared to that of blue galaxies) does not depend on environment while that of $k+a$ does. This suggests that the *environmental quenching timescale* is short, while other galaxies go from being star-forming to being passive on a long timescale independently of environment.

We have seen that green late types are twice as numerous as $k+a$'s. Starting from the logical assumption that both green and $k+a$ galaxies have a common progenitor among star-forming galaxies, and if we assume that the green phase lasts for about twice the time (of the order of 2 Gyr) of the $k+a$ visibility (~ 1 Gyr), we conclude that the short timescale and the long timescale SF "quenching" channels contribute about equally to the growth of the passive population.

Several authors have tried to estimate the "quenching timescale" using different approaches. A direct comparison is impossible because it strongly depends on how a "quenching or quenched" galaxy is defined. However, we report here some of the latest results as comparison reference.

Wetzel *et al.* (2013) found that satellite quenching is the dominant process for building up all quiescent galaxies at $M_* < 10^{10} M_\odot$. They proposed a "delayed-then-rapid" quenching scenario: satellite SFRs is unaffected for 2-4 Gyr after infall, after which star formation quenches rapidly, with an e-folding time of < 0.8 Gyr (see also McGee *et al.* 2009, 2011; De Lucia *et al.* 2012). These quenching time-scales are shorter for more massive satellites but do not depend on host halo mass.

Investigating objects in transition defined using a color-color diagram, Mok *et al.* (2013) proposed a much shorter quenching time scale with an e-folding time of < 0.5 Gyr. Schawinski *et al.* (2014), inspecting morphologies in addition to colors, concluding that only a small population of blue

early types move rapidly across the green valley after the morphologies are transformed from disk to spheroid and star formation is quenched rapidly ($\tau < 0.25$ Gyr). In contrast, the majority of BSF galaxies have significant disks, and they retain their late-type morphologies as their star formation rates decline very slowly ($\tau > 1$ Gyr).

Only Wheeler *et al.* (2014), studying a sample of dwarf galaxies, found much longer timescales (> 9.5 Gyr, a “slow starvation” scenario), concluding that the environmental processes triggering quenching must be highly inefficient.

8. SUMMARY AND CONCLUSIONS

Investigating a mass complete sample of galaxies drawn from the PM2GC (Calvi, Poggianti & Vulcani 2011), this paper focused mainly on two points: 1) characterizing the color (red, green, blue) and morphological (ellipticals, S0s, late types) transformation of galaxies as a function of the stellar mass and the environment and 2) studying the properties of the objects that are most likely in a transitional phase (green, RP late types, BSF early types), with the aim of understanding the evolutionary links between the different sub-populations.

Our analysis showed that the relative importance of the bulge and the disk seems to play an important role in galaxy transformations. We found that the fading and total or partial removal of the disk produces a morphological transition, so that BSF late types and green late types become BSF early types and green early types, respectively. On the other hand, a transition can occur even without a noticeable structural and morphological change: SFR can decline both in bulges and disks, producing a variation in color. In this way blue galaxies turn into green (when they are still forming stars, but a re-

duced rate) and red galaxies. Therefore, RP late-type galaxies descend from blue late types that have stopped forming stars at any epoch (retaining their morphology), going through either a short or a long green phase.

Our spectrophotometric model allowed us to better characterize the occurrence and duration of the green phase. In some cases galaxies can turn from blue to red quite quickly, going through a very short green phase (< 0.1 Gyr) hardly observable when considering only colors, but recognizable by their spectral $k + a$ features. In other cases green colors are not indicative of “quenching” processes. They are due to star formation histories declining with long timescales. These could be due either to “undisturbed” lognormal histories with τ typical of early-spirals or to long τ typical of late spirals that are quenched on the timescales of the order of at least 1 Gyr.

ACKNOWLEDGEMENTS

We thank the anonymous referee whose comments helped us to improve the readability of the paper. This work was supported by the World Premier International Research Center Initiative (WPI), MEXT, Japan. It was also supported by the Kakenhi Grant-in-Aid for Young Scientists (B)(26870140) from the Japan Society for the Promotion of Science (JSPS). The Millennium Galaxy Catalogue consists of imaging data from the Isaac Newton Telescope and spectroscopic data from the Anglo Australian Telescope, the ANU 2.3m, the ESO New Technology Telescope, the Telescopio Nazionale Galileo and the Gemini North Telescope. The survey has been supported through grants from the Particle Physics and Astronomy Research Council (UK) and the Australian Research Council (AUS).

REFERENCES

- Abadi, M. G., Moore, B., and Bower, R. G. 1999, *MNRAS*, 308, 947.
 Abraham, R. G. *et al.* 1994, *ApJ*, 432, 75.
 Abramson, L. E. *et al.* 2014, *ApJ*, 785, L36.
 Allen, P. D. *et al.* 2006, *MNRAS*, 371, 2.
 Bahé, Y. M. *et al.* 2013, *MNRAS*, 430, 3017.
 Baldry, I. K. *et al.* 2004, *ApJ*, 600, 681.
 Balogh, M. *et al.* 2004, *MNRAS*, 348, 1355.
 Balogh, M. L. *et al.* 1999, *ApJ*, 527, 54.
 Balogh, M. L., Navarro, J. F., and Morris, S. L. 2000a, *ApJ*, 540, 113.
 Balogh, M. L., Navarro, J. F., and Morris, S. L. 2000b, *ApJ*, 540, 113.
 Bamford, S. P. *et al.* 2009, *MNRAS*, 393, 1324.
 Bell, E. F. and de Jong, R. S. 2001, *ApJ*, 550, 212.
 Berlind, A. A. *et al.* 2006, *ApJS*, 167, 1.
 Blanton, M. R. *et al.* 2005, *ApJ*, 629, 143.
 Blanton, M. R. *et al.* 2003, *ApJ*, 594, 186.
 Bluck, A. F. L. *et al.* 2014, *MNRAS*, 441, 599.
 Boselli, A. and Gavazzi, G. 2006, *PASP*, 118, 517.
 Brinchmann, J. *et al.* 2004, *MNRAS*, 351, 1151.
 Brough, S. *et al.* 2008, *MNRAS*, 385, L103.
 Calvi, R. *et al.* 2012, *MNRAS*, 419, L14.
 Calvi, R., Poggianti, B. M., and Vulcani, B. 2011, *MNRAS*, 416, 727.
 Calvi, R. *et al.* 2013, *MNRAS*, 432, 3141.
 Carollo, C. M. *et al.* 2014, *ArXiv e-prints*.
 Christlein, D. and Zabludoff, A. I. 2005, *ApJ*, 621, 201.
 Cid Fernandes, R. *et al.* 2005, *MNRAS*, 358, 363.
 Cimatti, A. *et al.* 2008, *A&A*, 482, 21.
 Cole, S. *et al.* 2000, *MNRAS*, 319, 168.
 Cowie, L. L. *et al.* 1996, *AJ*, 112, 839.
 De Lucia, G. and Blaizot, J. 2007, *MNRAS*, 375, 2.
 De Lucia, G. *et al.* 2012, *MNRAS*, 423, 1277.
 Dekel, A. and Birnboim, Y. 2006, *MNRAS*, 368, 2.
 Dressler, A. *et al.* 1999, *ApJS*, 122, 51.
 Driver, S. P. *et al.* 2005, *MNRAS*, 360, 81.
 Eke, V. R. *et al.* 2004, *MNRAS*, 348, 866.
 Fasano, G. *et al.* 2012, *MNRAS*, 420, 926.
 Feldmann, R., Carollo, C. M., and Mayer, L. 2011, *ApJ*, 736, 88.
 Ferreras, I. *et al.* 2009, *MNRAS*, 395, 554.
 Finn, R. A. *et al.* 2005, *ApJ*, 630, 206.
 Font, A. S. *et al.* 2008, *MNRAS*, 389, 1619.
 Forbes, J., Krumholz, M., and Burkert, A. 2012, *ApJ*, 754, 48.
 Fritz, J. *et al.* 2007, *A&A*, 470, 137.
 Fritz, J. *et al.* 2011, *A&A*, 526, A45.
 Gallazzi, A. *et al.* 2009, *ApJ*, 690, 1883.
 Gavazzi, G., Pierini, D., and Boselli, A. 1996, *A&A*, 312, 397.
 Gehrels, N. 1986, *ApJ*, 303, 336.
 Gill, S. P. D., Knebe, A., and Gibson, B. K. 2005, *MNRAS*, 356, 1327.
 Gladders, M. D. *et al.* 2013, *ApJ*, 770, 64.
 Gunn, J. E. and Gott, III, J. R. 1972, *ApJ*, 176, 1.
 Hashimoto, Y. and Oemler, Jr., A. 1999, *ApJ*, 510, 609.
 Huchra, J. P. and Geller, M. J. 1982, *ApJ*, 257, 423.
 Kannappan, S. J., Guie, J. M., and Baker, A. J. 2009, *AJ*, 138, 579.
 Kauffmann, G. *et al.* 2003, *MNRAS*, 341, 54.
 Kauffmann, G. *et al.* 2004, *MNRAS*, 353, 713.
 Kawata, D. and Mulchaey, J. S. 2008, *ApJ*, 672, L103.
 Knobel, C. *et al.* 2009, *ApJ*, 697, 1842.
 Kovač, K. *et al.* 2010, *ApJ*, 718, 86.
 Kroupa, P. 2001, *MNRAS*, 322, 231.
 Lang, P. *et al.* 2014, *ArXiv e-prints*.
 Larson, R. B., Tinsley, B. M., and Caldwell, C. N. 1980, *ApJ*, 237, 692.
 Lewis, I. *et al.* 2002, *MNRAS*, 334, 673.
 Lin, L. *et al.* 2008, *ApJ*, 681, 232.
 Liske, J. *et al.* 2003, *MNRAS*, 344, 307.
 Masters, K. L. *et al.* 2010, *MNRAS*, 405, 783.
 McGee, S. L. *et al.* 2009, *MNRAS*, 400, 937.
 McGee, S. L. *et al.* 2011, *MNRAS*, 413, 996.
 Mok, A. *et al.* 2013, *MNRAS*, 431, 1090.
 Moore, B. *et al.* 1996, *Nature*, 379, 613.
 Omand, C. M. B., Balogh, M. L., and Poggianti, B. M. 2014, *MNRAS*, 440, 843.
 Park, C., Gott, J., and Choi, Y. 2007, in *American Astronomical Society Meeting Abstracts*, volume 39 of *Bulletin of the American Astronomical Society*, 771.
 Pasquali, A. *et al.* 2010, *MNRAS*, 407, 937.
 Pasquali, A. *et al.* 2009, *MNRAS*, 394, 38.

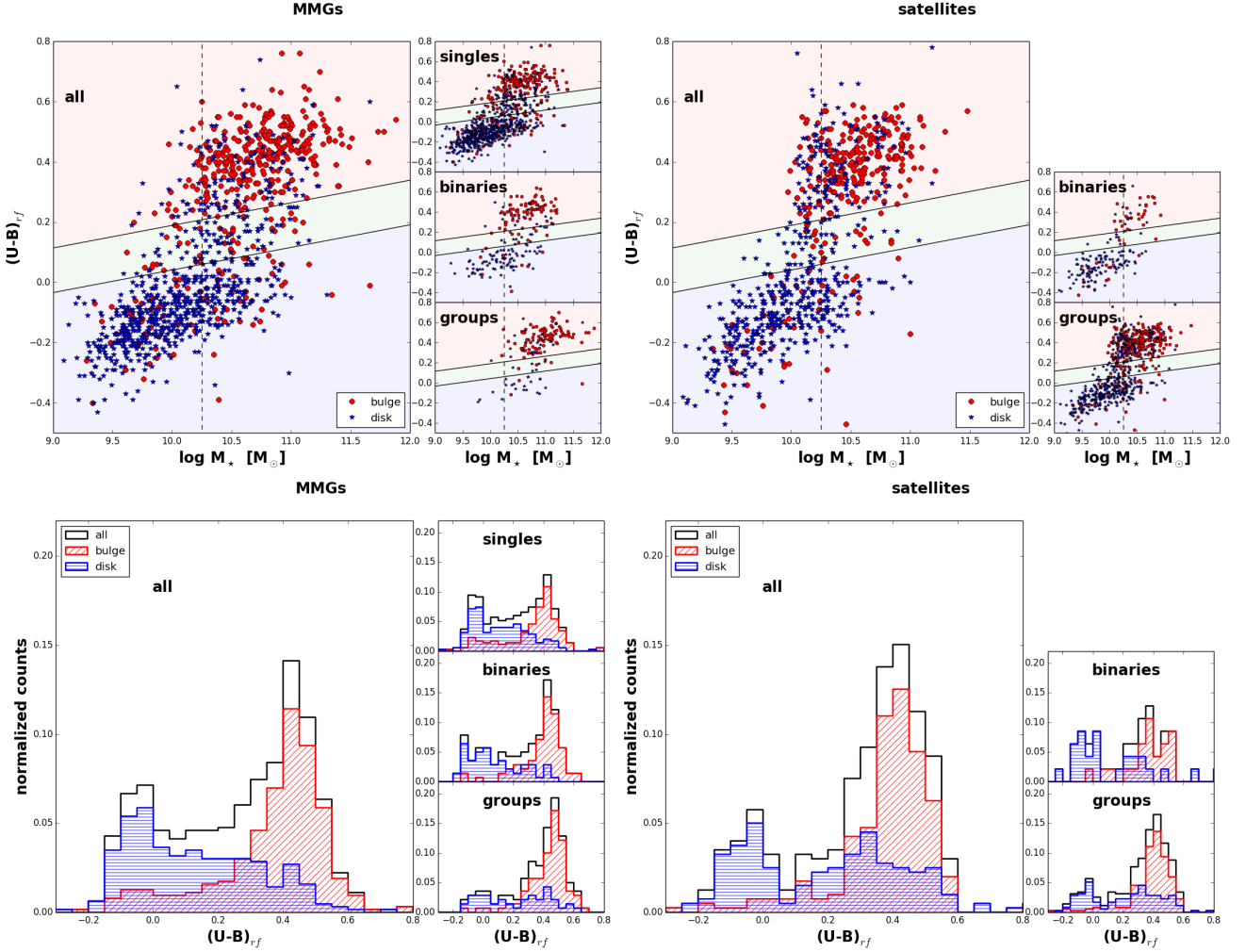


FIG. A1.— Rest frame $(U-B)_{rf}$ -mass relation (upper panels) and rest frame $(U-B)_{rf}$ color distribution (bottom panels) for galaxies of different types (left panels: MMGs, right panels: satellites) and Sérsic indexes in the different environments (shown in the smaller windows). Red lines and circles: bulges, blue lines and stars: disks. In the upper panels, the black dashed vertical line represents the mass completeness limit, the black solid line shows the separation between red, green and blue galaxies

Peng, Y.-j. *et al.* 2010, *ApJ*, 721, 193.
Pimbblet, K. A. 2008, *PASA*, 25, 176.
Poggianti, B. M. *et al.* 2013, *ApJ*, 762, 77.
Rider, P. R. 1960, *JASA*, 55, 148.
Rudnick, G. *et al.* 2003, *ApJ*, 599, 847.
Salpeter, E. E. 1955, *ApJ*, 121, 161.
Schawinski, K. *et al.* 2009, *MNRAS*, 396, 818.
Schawinski, K. *et al.* 2014, *MNRAS*, 440, 889.
Simard, L. *et al.* 2002, *ApJS*, 142, 1.
Skibba, R. A. *et al.* 2009, *MNRAS*, 399, 966.
Skibba, R. A. and Sheth, R. K. 2009, *MNRAS*, 392, 1080.
Skibba, R. A., Sheth, R. K., and Martino, M. C. 2007, *MNRAS*, 382, 1940.
Skibba, R. A. *et al.* 2011, *MNRAS*, 410, 417.
Smith, R. J. *et al.* 2012, *MNRAS*, 419, 3167.
Tanaka, M. *et al.* 2004, *AJ*, 128, 2677.
Taylor, E. N. *et al.* 2009, *ApJS*, 183, 295.
Tojeiro, R. *et al.* 2013, *MNRAS*, 432, 359.

van den Bosch, F. C. *et al.* 2008, *MNRAS*, 387, 79.
van der Wel, A. *et al.* 2009, *ApJ*, 706, L120.
von der Linden, A. *et al.* 2010, *MNRAS*, 404, 1231.
Vulcani, B. *et al.* 2014, *ApJ*, 788, 57.
Walker, I. R., Mihos, J. C., and Hernquist, L. 1996, *ApJ*, 460, 121.
Wang, H., Mo, H. J., and Jing, Y. P. 2009, *MNRAS*, 396, 2249.
Weinmann, S. M. *et al.* 2009, *MNRAS*, 394, 1213.
Weinmann, S. M., van den Bosch, F. C., and Pasquali, A. 2011. The Dependence of Low Redshift Galaxy Properties on Environment, 29.
Weinmann, S. M. *et al.* 2006, *MNRAS*, 366, 2.
Wetzel, A. R. *et al.* 2014, *MNRAS*, 439, 2687.
Wetzel, A. R. *et al.* 2013, *MNRAS*, 432, 336.
Wheeler, C. *et al.* 2014, *ArXiv e-prints*.
Wolf, C. *et al.* 2009, *MNRAS*, 393, 1302.

APPENDIX

TRENDS WITH SÉRSIC INDEXES

In this paper we have investigated the relationship between color and morphology. In this Appendix we show that adopting the Sérsic index instead of morphology to distinguish between the sub-populations overall gives similar results, even though the analysis of the morphologies is more detailed.

We separate the sample into bulge-dominated galaxies ($n > 2.5$ - hereafter simply “bulges”) and disk-dominated galaxies ($n < 2.5$ - hereafter simply “disks”). Figure A1 shows the same as Fig.2. Bulges are most likely red and more massive, while disks tend to be bluer. As shown in Tab.A1, bulge and disk fractions depend on the environment: for both MMGs and satellites, bulges

TABLE A1
PERCENTAGE OF GALAXIES OF DIFFERENT TYPES ABOVE THE STELLAR MASS COMPLETENESS LIMIT IN DIFFERENT ENVIRONMENTS.

MOST MASSIVE GALAXIES								
	ALL GALAXIES		SINGLE GALAXIES		BINARY SYSTEMS		GROUPS	
	<i>bulge</i>	<i>disk</i>	<i>bulge</i>	<i>disk</i>	<i>bulge</i>	<i>disk</i>	<i>bulge</i>	<i>disk</i>
COLOR								
<i>all</i>	54±3	46±3	49±4	51±4	56±6	44±6	67±6	33±6
<i>red</i>	45±3	11±2	37±4	15±3	48±6	10±4	62±6	17±5
<i>green</i>	3±1	9±2	3±1	12±2	5±3	8±4	3±2	4±3
<i>blue</i>	5±1	21±2	8±2	23±3	2±2	26±5	2±2	11±4
SATELLITES								
	ALL GALAXIES		SINGLE GALAXIES		BINARY SYSTEMS		GROUPS	
	<i>bulge</i>	<i>disk</i>	<i>bulge</i>	<i>disk</i>	<i>bulge</i>	<i>disk</i>	<i>bulge</i>	<i>disk</i>
COLOR								
<i>all</i>	57±3	43±3	—	—	47±11	53±11	59±4	42±4
<i>red</i>	51±4	23±3	—	—	40±11	19±9	52±4	22±3
<i>green</i>	3±1	5±2	—	—	4±5	4±5	3±1	5±2
<i>blue</i>	3±1	16±2	—	—	2±4	30±10	3±1	14±3

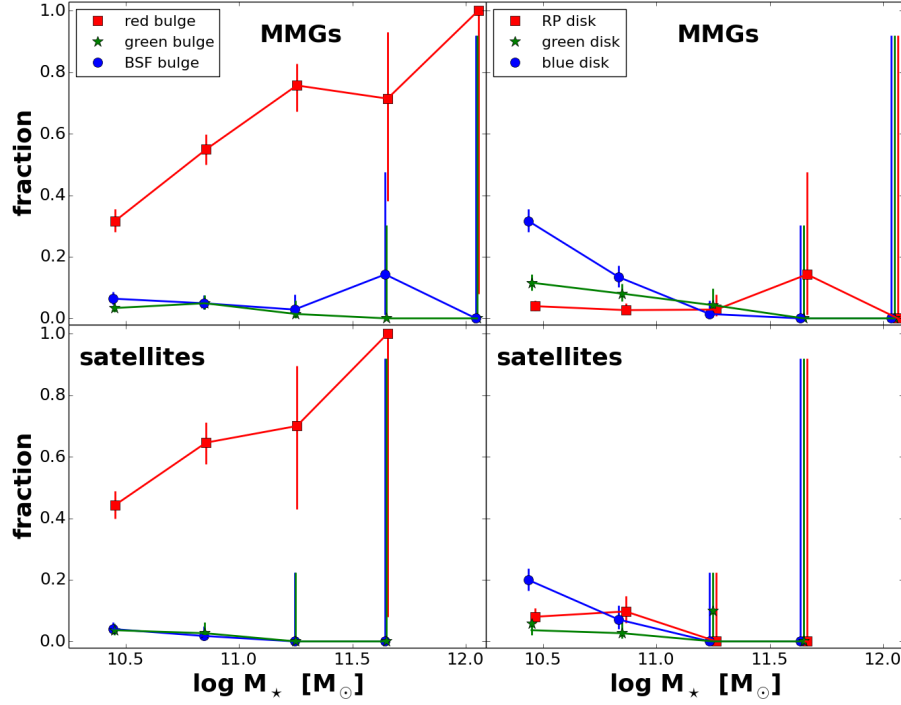


FIG. A2.— Fraction of galaxies as a function of stellar mass for MMGs (upper panels) and satellites (bottom panels), when a color+SSFR+Sérsic index cut is adopted. Left panels: early types, as indicated in the labels. Right panels: late types, as indicated in the labels. Errors are defined as binomial errors (Gehrels 1986).

are more common in groups than in single systems. However, in a given environment, fractions differ for satellites and MMGs only in groups, with MMGs hosting a higher fraction ($\sim 70\%$) of bulges than satellites ($\sim 60\%$). Both for MMGs and satellites and in all environments, the distribution of disks resembles the one presented for late types and that of bulges that of the sum of ellipticals+S0s.

Figure A2 shows the same as Fig.3. In both MMGs and satellites, blue and green disks show similar trends to blue and green late types, that is they are more frequent at low masses than at higher. In MMGs, together, they dominate the total population at low masses, while in satellites red bulges always dominate, with their importance increasing with increasing mass. In general, red bulges resemble red early types. We note that in satellites the contribution of red bulges increases from 40% to 100% without showing any dip. This might suggest that the weird trend seen in red early and late types is due to galaxies that are morphologically classified as late, but have a non negligible bulge. In both classes, trends for BSF bulges, RP disks and green bulges are almost flat. All these galaxies are absent only in the highest mass bin. Each sub-population represents $\leq 15\%$ of the total population.

Focusing on groups, Figure A3 shows the same as Figure 6. Both at low and high masses, within the errors, trends for satellites and MMGs are compatible. At low masses, the incidence of red bulges (which dominate close to the group centers) seems to decrease at large distances. In contrast, the fraction of blue and green disks and BSF disks slightly increases. Green bulges are almost absent at all distances. At higher masses, both in MMGs and satellites, red bulges dominate at all distances ($>60\%$), and

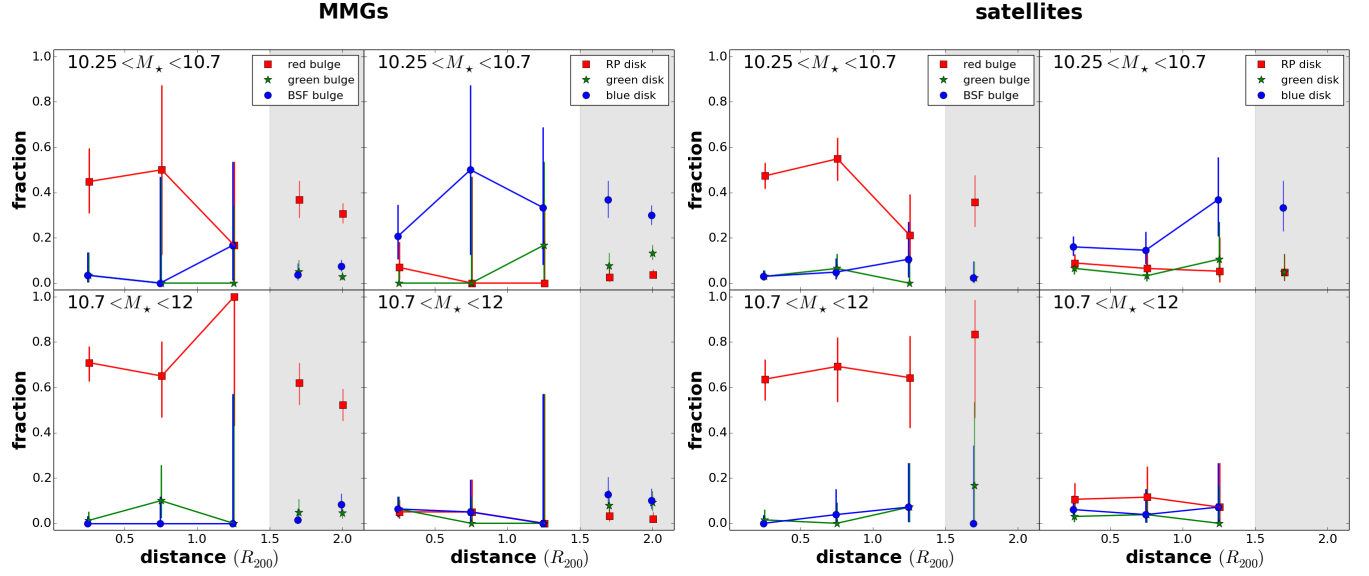


FIG. A3.— Fraction of galaxies as a function of group-centric distances in bins of stellar mass, when a color+SSFR+Sérsic index cut is adopted. Left panel: MMGs. Right panel: satellites. Left panels: $\log M_*/M_\odot < 10.7$, right panel: $\log M_*/M_\odot > 10.7$. Colors and symbols are as in Fig.A2. Grey area represent galaxies that are not in groups, i.e. binary systems (placed at $r/R_{200}=1.7$) and single galaxies (placed at $r/R_{200}=2$). Errors are defined as binomial errors (Gehrels 1986).

TABLE B1
CHARACTERISTIC NUMBERS OF ELLIPTICALS AND S0S, COMPARED TO NORMAL GALAXIES OF THE SAME MORPHOLOGY.

Quantity	ellipticals			S0s		
	red	green	BSF	red	green	BSF
number	295	15	18	281	36	32
$\langle B_{Vega} \rangle$	-19.97 ± 0.05	-19.8 ± 0.2	-20.4 ± 0.1	-19.87 ± 0.05	-19.8 ± 0.1	-20.28 ± 0.09
$\langle \log M_*/M_\odot \rangle$	10.66 ± 0.05	10.4 ± 0.1	10.40 ± 0.06	10.62 ± 0.05	10.48 ± 0.06	10.39 ± 0.07
$\langle SFR \rangle (M_\odot \text{yr}^{-1})$	0 ± 0	1 ± 1	4.7 ± 0.7	0 ± 0	1.8 ± 0.5	3 ± 1
$\langle SSFR \rangle^\alpha (yr^{-1})$	$(8 \pm 5) 10^{-12}$	$(3 \pm 3) 10^{-11}$	$(1.5 \pm 0.2) 10^{-10}$	$(9 \pm 3) 10^{-12}$	$(4 \pm 1) 10^{-11}$	$(7 \pm 3) 10^{-11}$
$\langle n \rangle$	3.4 ± 0.1	2.8 ± 0.4	2.3 ± 0.5	3.3 ± 0.1	2.7 ± 0.4	1.8 ± 0.4
$\langle B/T \rangle$	0.61 ± 0.02	0.58 ± 0.08	0.7 ± 0.1	0.51 ± 0.02	0.52 ± 0.06	0.25 ± 0.08
$\langle R_e (bulge) \rangle (\text{kpc})$	1.13 ± 0.07	0.9 ± 0.2	1.2 ± 0.3	1.09 ± 0.08	1.2 ± 0.3	1.2 ± 0.2
$\langle R_e (disk) \rangle (\text{kpc})$	2.4 ± 0.1	2.2 ± 0.4	1.5 ± 0.2	2.1 ± 0.1	2.0 ± 0.2	2.0 ± 0.2
$\langle (u-r) \text{ bulge} \rangle^\beta$	2.66 ± 0.04	2.2 ± 0.1	1.95 ± 0.09	2.65 ± 0.01	2.3 ± 0.1	1.91 ± 0.06
$\langle (u-r) \text{ disk} \rangle^\beta$	2.52 ± 0.05	2.2 ± 0.3	2.0 ± 0.3	2.53 ± 0.06	2.3 ± 0.1	1.9 ± 0.1

^α Values computed only with galaxies with $SSFR \neq 0$

^β Colors are in the AB system

their fraction increases with distance. In contrast, the other three classes of objects show slightly declining trends. In the non group environments, in both mass bins fractions are similar to those of group outskirts, given the large uncertainties.

ELLITPICALS AND S0S

In the main text we have presented results for ellipticals and S0s together, nonetheless it is known that they are characterized by different properties. Table B1 presents the characteristic numbers for the two populations.

Red ellipticals and S0s differ especially in the B/T ratio, with the former being more bulge dominated than the latter. Similar discrepancies are found also for the objects in transitions. In addition, we note that BSF ellipticals are more star-forming than S0s, showing on average higher values of SFR and SSFR.